FINITE DIFFERENCE APPROXIMATIONS OF VARIOUS STEKLOV EIGENVALUE PROBLEMS

A THESIS SUBMITTED TO
THE GRADUATE SCHOOL OF NATURAL AND APPLIED SCIENCES
OF
MIDDLE EAST TECHNICAL UNIVERSITY

BY

MÜCAHİT ÖZALP

IN PARTIAL FULFILLMENT OF THE REQUIREMENTS
FOR
THE DEGREE OF MASTER OF SCIENCE
IN
MATHEMATICS

AUGUST 2022

Approval of the thesis:

FINITE DIFFERENCE APPROXIMATIONS OF VARIOUS STEKLOV EIGENVALUE PROBLEMS

submitted by **MÜCAHİT ÖZALP** in partial fulfillment of the requirements for the degree of **Master of Science in Mathematics Department, Middle East Technical University** by,

Prof. Dr. Halil Kalıpçılar
Dean, Graduate School of **Natural and Applied Sciences** _____

Prof. Dr. Yıldıray Ozan
Head of Department, **Mathematics** _____

Prof. Dr. Canan Bozkaya
Supervisor, **Department of Mathematics, METU** _____

Assoc. Prof. Dr. Önder Türk
Co-supervisor, **Institute of Applied Mathematics, METU** _____

Examining Committee Members:

Prof. Dr. Songül Kaya Merdan
Department of Mathematics, METU _____

Prof. Dr. Canan Bozkaya
Department of Mathematics, METU _____

Prof. Dr. Ayhan Aydın
Department of Mathematics, Atılım University _____

Date: 26.08.2022

I hereby declare that all information in this document has been obtained and presented in accordance with academic rules and ethical conduct. I also declare that, as required by these rules and conduct, I have fully cited and referenced all material and results that are not original to this work.

Name, Surname: MÜCAHİT ÖZALP

Signature :

ABSTRACT

FINITE DIFFERENCE APPROXIMATIONS OF VARIOUS STEKLOV EIGENVALUE PROBLEMS

ÖZALP, MÜCAHİT
M.S., Department of Mathematics
Supervisor: Prof. Dr. Canan Bozkaya
Co-Supervisor: Assoc. Prof. Dr. Önder Türk

August 2022, 77 pages

In this thesis, the finite difference method (FDM) is employed to numerically solve differently defined Steklov eigenvalue problems (EVPs) that are characterized by the existence of a spectral parameter on the whole or a part of the domain boundary. The FDM approximation of the Laplace EVP is also considered due to the fact that the defining differential operator in a Steklov EVP is the Laplace operator. The fundamentals of FDM are covered and their applications on some BVPs involving Laplace operator are discussed. Using Taylor's series expansions, approximation formulas for the derivatives of the functions are provided, with varying degrees of accuracy. To validate our formulation of FDM, the second and fourth order formulas are first used to approximate two test problems for which the analytical solutions are known, namely, the Poisson problem and the Laplace EVP. It is demonstrated that the solutions from the FDM agree well with the exact ones and that the results from the fourth order scheme are superior to those from the second order one. Secondly, we consider two Steklov eigenvalue problems that are distinct from each other by the associated boundary conditions. Specifically, the standard Steklov EVP with a mixed

type boundary condition involving a spectral parameter is analyzed as the first problem, whereas in the second problem, the boundary of the computational domain is divided into two parts; one with Neumann type boundary condition and the other with spectral boundary condition. The discretization of the problem is performed by several orders of finite difference formulas for the first time to the best of our knowledge. The agreement between the approximate and exact eigenfunctions is shown using contour plots, and the rate of convergence of the approximate eigenvalues to the reference ones is given. It has been noted that the use of higher order finite difference approximations -of at least second order- for not only the differential equation but also the boundary conditions advances the rate of convergence. Consequently, the present study demonstrates how a second-order convergence can be acquired by the application of fourth-order finite difference formulas for both the differential operator and the accompanying boundary conditions.

Keywords: Steklov eigenvalue problems, Laplace eigenvalue problem, finite difference method, second and fourth order schemes

ÖZ

ÇEŞİTLİ STEKLOV ÖZDEĞER PROBLEMLERİNİN SONLU FARKLAR YAKLAŞIMLARI

ÖZALP, MÜCAHİT
Yüksek Lisans, Matematik Bölümü
Tez Yöneticisi: Prof. Dr. Canan Bozkaya
Ortak Tez Yöneticisi: Doç. Dr. Önder Türk

Ağustos 2022 , 77 sayfa

Bu tezde, tanım bölgesinin tamamında ya da bir kısmında spektral parametrenin varlığı ile karakterize edilen, farklı şekilde tanımlanan Steklov özdeğer problemlerini (ÖDP) nümerik olarak çözmek için sonlu farklar yönetimi (SFY) kullanılmıştır. Steklov ÖDPde diferansiyel operatör Laplace opetatörü olduğundan, Laplace ÖDPnin SFY yaklaşımı da ele alınmıştır. SFYnin temelleri verilmiş ve Laplace operatörünü içeren bazı sınır değer problemleri üzerindeki uygulamaları tartışılmıştır. Taylor seri açılımları kullanılarak fonksiyonların türevleri için yaklaşım formülleri, değişen doğruluk dereceleri ile birlikte verilmiştir. SFY formülasyonumuzu doğrulamak için ilk önce, ikinci ve dördüncü mertebeden formüller, Poisson problemi ve Laplace ÖDP gibi analitik çözümleri bilinen iki test probleminin yaklaşık çözümünü elde etmek için kullanılmıştır. SFY çözümlerinin gerçek çözümler ile iyi bir şekilde uyuştuğu ve dördüncü mertebe şemasından elde edilen sonuçların ikinci mertebeden elde edilenlerden daha üstün olduğu gösterilmiştir. İkinci olarak, farklı sınır koşullarına sahip iki Steklov özdeğer problemleri ele alınmıştır. İlk olarak, tüm sınırda bir spektral pa-

rametre içeren karma tip sınır koşuluna sahip standart Steklov ÖDP analiz edilmiş, ikinci problemde ise, bölge sınırı iki bölüme ayrılmıştır; öyle ki sınırın bir bölümü Neumann tipi sınır koşuluna diğer bölümü ise spektral sınır koşuluna sahiptir. Yazarların bilgisi dahilinde, farklı dereceden fark formülleri kullanılarak Steklov özdeğer problemlerinin ayrıklaştırılması ilk kez yapılmıştır. Yaklaşık ve gerçek özfonksiyonlar arasındaki uyum eşyükselti eğrileri kullanılarak gösterilmiş ve yaklaşık özdeğerlerin referans özdeğerlere yakınsama oranı verilmiştir. Sadece diferansiyel denklem için değil, aynı zamanda sınır koşulları için de daha yüksek mertebeden sonlu fark yaklaşımlarının kullanılmasıyla- en az ikinci mertebeden- yakınsama hızının arttığı gözlenmiştir. Sonuç olarak, hem diferansiyel operatörüne hem de beraberindeki sınır koşullarına dördüncü mertebeden sonlu fark formüllerinin uygulanmasıyla, ikinci dereceden bir yakınsaklığın nasıl elde edilebileceği bu çalışmada gösterilmiştir.

Anahtar Kelimeler: Steklov özdeğer problemleri, Laplace özdeğer problemi, sonlu farklar metodu, ikinci ve dördüncü mertebeden şemalar

To my parents, Semra and Bekir,
my brother Burak

ACKNOWLEDGMENTS

First, I want to sincerely thank my supervisor, Prof. Dr. Canan Bozkaya and my co-supervisor, Assoc. Dr. Önder Türk, for all their help, patience, and valuable contributions throughout the completion of this thesis.

I would also like to thank the members of my defense committee, Prof. Dr. Songül Kaya Merdan and Prof. Dr. Ayhan Aydın.

No mention of my close friends Begüm, Cansel, Derya, Emre, Emrehan, Engin, Eren, Evindar, Furkan, Gökberk, Gökhan, Mehmet, Metehan, Muhammed, Mustafa, Salih, Yonca, Ümitcan, İdris, Şenay, and my calculus students would be complete without acknowledgment of their support and contributions to keeping my mentality secure.

Above all else, I want to express my gratitude to my parents, Semra and Bekir, as well as my brother Burak, for their contiuning support throughout my life.

TABLE OF CONTENTS

LIST OF TABLES

TABLES

LIST OF FIGURES

FIGURES

CHAPTER 1

INTRODUCTION

Partial differential equations (PDEs) are mathematical equations having an unknown function, two or more independent variables, the partial derivatives of the unknown function with respect to the independent variables and a specific domain. Fluid mechanics, electromagnetics, and heat and mass transfer are all real-world applications of physics and engineering that are all modelled by appropriate PDEs under certain assumptions. The partial differential equations are classified into three types: elliptic, parabolic, and hyperbolic PDEs. Each type has certain properties that aid in determining whether a method is appropriate for the problem modelled by the PDE, or the solution depends on the equation and its type.

Boundary value problems (BVPs) are formed by a PDE and a few boundary conditions, which are some necessary constraints on the boundary $\partial\Omega$ of the domain Ω. In fact, BVPs are a set of equations that include the derivatives of the unknown function. Examples of BVPs that are investigated in the present thesis are the Laplace and Steklov eigenvalue problems (EVPs), which are both modelled by elliptic type PDEs with appropriate boundary conditions of different types, namely, Dirichlet type ($u = f(x, y)$ on $\partial\Omega$ with f is a given continuous function), Neumann type ($\partial u/\partial n = f(x, y)$ on $\partial\Omega$ where $\partial u/\partial n$ shows the normal derivative of u in the outward normal direction on the boundary) and Robin (mixed) type ($\alpha u + \beta\partial u/\partial n = f(x, y)$ on $\partial\Omega$).

The eigenvalue problem is defined as finding the eigensolutions (λ, u) such that

$$\mathcal{L}f = \lambda u$$

where λ is a complex number which is said to be an eigenvalue of a linear operator $\mathcal{L}$, and the non-zero u is called an eigenfunction that is associated with λ in a vector

space. Eigenvalues are often introduced in the context of linear algebra or matrix theory. But historically, they emerged from the study of differential equations and quadratic forms. Early in the 19*th* century, Augustin-Louis Cauchy generalized his work to encompass arbitrary dimensions after realizing how it could be used to categorize the quadric surfaces [1]. Eigenvalues and eigenvectors have a wide range of uses in including stability analysis, vibration analysis, atomic orbitals, facial recognition, and matrix diagonalization [2, 3].

A Steklov eigenvalue problem, which is one of the popular elliptic type problems, arises in the study of many mathematical physics fields such as the vibration modes of a structure in contact with an incompressible fluid [4], mechanical oscillators immersed in a viscous fluid [5], surface waves [6] and electronic structure calculations [7]. The problem has also daily life applications. In fact, in a recent research, it was used to explain why spilling coffee from a mug is simpler than spilling wine from a snifter by Krechetnikov and Mayer [8]. They used a suitable mixed Steklov EVP, usually known as the sloshing problem, to represent the coffee's oscillation.

In December 1895, Steklov presented Steklov eigenvalue problem in his speech at a session of the Kharkov Mathematical Society [4]. In the present day, it is originally mentioned as Steklov problem but on some occasions it is used as Stekloff problem. There has been significant advancement in the analysis of the Steklov EVPs over the past few years, and some interesting problems have indeed emerged. Now, we continue with emphasizing the motivation of the present thesis. For applications to electrical impedance tomography, which is employed in geophysical and medical imaging, the study of voltage to current map is crucial [9]. Additionally, the mathematical analysis of photonic crystals heavily relies on the Steklov spectrum [10]. Studying the nodal domains and nodal sets of Steklov eigenfunctions also presents new difficulties. Understanding whether the nodal lines of Steklov eigenfunctions are dense at the wave-length scale, which is a fundamental characteristic of the zeros of Laplace eigenfunctions, is one of the interesting problems [11].

As it is well-known finding the analytical solutions of PDEs is a challenging task or even mostly impossible. For example, there are only a few cases in which analytical solutions to Steklov eigenvalue problems exist. It might not be possible to predict

the response using the existing methods as the problem equation becomes more complicated due to geometry or material complexity. Thus, in such cases, the use of numerical methods provides a good sight to understand the behavior of the related solution.

Finite difference method (FDM) is one of the effective numerical methods for the solution of partial differential equations. The method proceeds by replacing the derivatives in the equation of the problem with finite difference approximations derived by using Taylor's series expansion around a grid point. The domain of the problem for the two-dimensional case is divided into partitions in x and y-directions, and the division results in grid points on the domain. Approximating the derivatives in the differential equation yields the difference equation which can be written as a system of algebraic equations to be solved instead of a differential equation.

In this thesis, we focus on the solution of various Steklov EVPs by using FDM. Nevertheless, we start our investigation by the so called Laplace eigenvalue problem in a square region for which the exact solution is available in order to construct and validate our numerical FDM codes. Then, we extend our numerical simulations for the Steklov eigenvalue problems with different boundary conditions defined on a square computational domain. The results are mainly presented in terms of convergence behavior of the approximate eigenvalues to the reference or exact ones, and contour plots of eigenfunctions.

1.1 Literature Survey

Approximation of the eigenvalue problems has great value in many fields of science, such as electronic structure calculations of materials [7], machine learning [12] and magnetohydrodynamics [13]. The Laplace eigenvalue problem and Steklov eigenvalue problem are the two significant eigenvalue problems that have received comprehensive study using some numerical techniques. In Section 1.1.a and Section 1.1.b, the studies on the solutions of Laplace and Steklov eigenvalue problems by using numerical techniques different from FDM are given, and finally the studies on the finite difference approximations of eigenvalue problems are given in Section 1.1.c.

1.1.a Numerical Methods Applied to Laplace Eigenvalue Problems

One of the fundamental concepts in many fields of mathematics and physics, such as computer science, spectral theory, probability, dynamical systems, quantum billiards, quantum mechanics, the theory of acoustic and quantum waveguides, is the Laplace eigenvalue problem [14]. There are numerous works that discuss the analysis in broad frameworks where issues like stability, convergence aspects, and error estimates are concerned. Different types of the problem exist according to the taken boundary conditions and the problem domain.

A boundary element method for the Laplace eigenvalue problem with Dirichlet type boundary conditions is considered by Steinbach and Unger [15]. As a model problem, they studied the problem on a cubic domain, and compared the solutions obtained by boundary element and finite element methods. The results showed that the methods gave different convergence rates. In [16], Gottlieb worked on the asymptotic expansions of the Laplace eigenvalue problem under the Neumann and mixed type boundary conditions. Both two and three-dimensional cases, specifically narrow annulus, annular cylinder and thin concentric spherical cavity, were considered. In [17], Laplace eigenvalue problem in mixed form was solved by the virtual element method. The results for the unit square and unit disk revealed that an optimal convergence order was obtained. Lederer [18] worked on the derivation of an optimal and asymptotically exact a posteriori error estimates for the approximation of the Laplace eigenvalue problem. First, he applied the hypercircle methods created for the mixed Raviart-Thomas finite element eigenvalue approximations. Additionally, he made use of the post-processings for eigenvalue and eigenfunction based on mixed approximations with the Brezzi-Douglas-Marini finite element. To validate his theoretical findings, he discussed the convergence of some numerical examples on unit square and L-shaped domains. In [19], for the Laplace-Beltrami eigenvalue problem, Lu and Xu suggested a brand-new trace finite element approach which was first developed by Olshanskii, Reusken and Grade [20]. In their work, they focused on the trace finite element method, specifically on unit spherical and tooth-shaped surfaces. FuSheng et.al. [21] enriched the Crouzerix-Raviart element, and extended a special element, to obtain the lower bounds of the eigenvalues of the Laplace eigenvalue problem. Moreover, they used conforming finite elements to get the upper bounds for

the eigenvalues in the postprocessing process. Liu and Oishi [22] also used the finite element method to bind the leading eigenvalues of the Laplace EVP over polygonal domains. They demonstrated efficiency and flexibility of their algorithm on triangle domain, L-shaped and unit square domains with a crack.

1.1.b Numerical Methods Applied to Steklov Eigenvalue Problems

The Steklov EVP is widely investigated by using various numerical approaches, many of which depending on the finite element method.

Monk and Zhang [23] approximated the Steklov eigenvalue problem by hybridizable discontinuous Galerkin method. They demonstrated the optimal rates of convergence for the eigenvalues and eigenfunctions of the sloshing problem. In [24], spectral indicator method was applied by using the Lagrange finite element method for the discretization, and spectral perturbation theory was employed for the compact operators. Armentano and Lombardi [25] analyzed the approximation of Steklov eigenvalue problem in a plane domain with an external cusp by piece-wise linear finite elements in the discretization of the domain. Li et al. [26] studied the nonconforming finite elements for the solution of Steklov eigenvalue problems both on the convex and concave domains. According to their analysis, for a special and enriched Crouzeix- Raviart elements, they obtained lower bounds of the eigenvalues. Mora et al. [27] focused on a posteriori error analysis of a virtual element method (VEM) for Steklov EVP. They, further, reported the results of the two numerical test problems conducted in the work [28], and claimed that the virtual element method had the advantage of using general polygonal meshes. This showed that the adaptive VEM performed marginally better than the adaptive finite element method in their first test where they obtained a second order $O(h^2)$ convergence rate of the eigenvalues for sloshing problem in a square domain. The second test was performed in a unit square from which an equilateral triangle is subtracted. They obtained the convergence rate of order $O(h^{6/5})$. Bi et al. [29] approximated a fourth order Steklov eigenvalue problem with conforming finite element method. They obtained the solutions by using Bogner-Fox-Schmit and Morley elements on a square domain. Andreev and Todorov [30] worked on the isoparametric variant of the finite element method to approxi-

mate the Steklov EVP. They considered the numerical example over the quarter of the unit disc in the first quadrant with Neumann and Dirichlet boundary conditions. Moreover, for the non-self-adjoint Steklov eigenvalue problem resulting from inverse scattering, Xu et al. [31] introduced an asymptotically exact a posteriori error estimator, and its applications in adaptive finite element method were also studied. They demonstrated numerical examples on L-shaped domain. On the other hand, Yue et al. [32] proposed a new type of multilevel method for solving Steklov eigenvalue problem based on Newton's method. They proved that the iteration scheme yielded linear convergence rate on both unit square and dumbbell-shaped domains. Finally, a recent study on the dual reciprocity boundary element method for the solution of Steklov eigenvalue problem was given in the work of Türk [33]. He investigated the convergence of the method for several cases including selfadjoint and non-selfadjoint operators. For a variety of mixed Steklov eigenvalue problems on various domains, efficient approximations to the solution were demonstrated.

1.1.c FDM Applied to Various Eigenvalue Problems

As given in Sections 1.1.a and 1.1.b, the numerical solutions for the Laplace and Steklov eigenvalue problems mainly uses various type of finite element approaches. In this section, some finite difference studies on the solution of some eigenvalue problems are listed.

Aboud [34] investigated numerically nonlinear second order eigenvalue problems in both one-dimensional bounded and unbounded domains, and compared the finite difference discretization and spectral method solutions. In [35], Carasso studied the convergence of a centred finite difference approximation to nonselfadjoint Strum-Liouville eigenvalue problem, and he demonstrated the rate of convergence was order of $O(\Delta x^2)$. Usmani [36] approximated the eigenvalues of a two point boundary value problem associated with a fourth order linear differential equation by some new finite difference methods of order two and four. Motivated by the Usmani's work, Chawla and Shivakumar [37] derived a higher order symmetric method and applied it for computing eigenvalues of Strum-Lioville problems. Sajavicius [38] took into account the eigenvalue problems for the second order finite difference operators with nonlocal

coupled boundary conditions in one and two-dimensions. He established the requirements for the existence of complex, positive, negative, and zero eigenvalues. O'Brien et al. [39] performed a local meshless radial basis function finite difference method on the elliptic Helmholtz eigenvalue problem with a periodic domain, in which the numerical results displayed excellent agreement with the analytical solutions within an error of less than 10^{-6}. On the other hand, Kuttler [40] studied the finite difference approximations of the Laplace eigenvalue problem. As the mesh width tends to zero, he provided asymptotic estimates for the error. Later, Kuttler gave upper and lower bounds for eigenvalues by finite differences on his another work, [41]. Veidinger [42] also worked on the eigenvalues and eigenfunctions of the Laplace operator with finite difference method. He used five point difference operator to approximate the Laplace operator as in the present thesis. It is seen that there exists a few studies on the FDM solution of Laplace EVP, and there is no FDM studies on the Steklov EVPs to the best of our knowledge. This establishes the basis for our reasoning behind the FDM solutions of the Laplace and Steklov EVPs in the present thesis.

1.2 Plan of the Thesis

The fundamentals of finite difference method are discussed in Chapter 2 along with their applications to a few BVPs involving the Laplace operator. A derivation of some of the FDM approximation formulas based on Taylor's series expansions is introduced. Then, in order to validate our numerical simulations and computer code, we apply these formulas to two test problems with existing theoretical solutions. First, the two-dimensional Poisson problem on a square domain is taken into account by roughly approximating the second order derivative terms in the Laplace operator with second and fourth order central difference formulas using equal length of mesh grids. Discretization of the boundary is performed by using a suitable approximation formula. The exact and FDM solutions to the Poisson problem exhibit high levels of agreement. Then, the Laplace eigenvalue problem which is the problem that most closely resembles the main problem of the thesis, namely the Steklov EVP, is approximated using a second order central and a compact fourth order difference formulas. The analysis is carried out for the convergence of the normalized error in the

eigenvalues. Then, a good agreement in the contour plots of the exact and numerical eigenfunctions is obtained in the computational domain.

Chapter 3 presents the finite difference method solution of Steklov eigenvalue problems. Two Steklov eigenvalue problems, that are distinct from one another according to the boundary conditions, are taken into consideration. In particular, as a first problem the standard Steklov EVP with a mixed type boundary condition involving a spectral parameter is analyzed, while in the second problem the computational domain boundary is divided into two parts, one with Neumann and the other with spectral boundary conditions. The two problems are discretized using different orders of finite difference formulas. The obtained linear system of equations, which is an eigenvalue problem (or a generalized EVP), is integrated into a sparse matrix eigenvalue solver in MATLAB code. If the analytical solutions are available, the numerical results are compared to them; otherwise, they are compared to reference values, which are the best numerical results that can be obtained by FDM on our computer. Using contour plots, the agreement between the approximate and exact eigenfunctions is displayed, and the rate at which the approximate eigenvalues converge to the reference ones is investigated.

1.3 Contributions in the Thesis

In this thesis, FDM is regarded as a method for obtaining approximations to the Laplace and Steklov EVPs. Although there are some works on Laplace eigenvalue problem with FDM, the standard Steklov EVP and the mixed type Steklov EVP have been analyzed by using FDM for the first time in this thesis to the best of the author's knowledge. When the boundary conditions are approximated using a combination of first and second order finite difference formulas, one can obtain a linear (first order) convergence behavior for eigenvalues. On the other hand, using a combination of second and fourth order difference formulas for the approximation of boundary conditions, which involve the spectral parameter, results in a quadratic convergence behavior in the eigenvalues of Steklov EVP. Thus, FDM is a practical and effective numerical method for solving Steklov eigenvalue problems because it is simple to apply (on simple geometries) and produces a reasonable convergence rate of second

order for the eigenvalues.

CHAPTER 2

THE FINITE DIFFERENCE METHOD AND ITS APPLICATIONS WITH THE LAPLACE OPERATOR

The basics of FDM and their applications on some BVPs involving Laplace operator are reviewed in this chapter. FDM primarily focuses on producing approximation formulas for the derivatives of functions of any order with varying degrees of accuracy. In this regard, the derivation of some of these approximation formulas using Taylor's series expansions are presented in Section 2.1. Then, in Section 2.2, the application of these formulas is performed to two test problems for which theoretical solutions are known in order to validate our FDM computer code. To begin, the two-dimensional Poisson problem is handled by approximating the terms in the Laplace operator with second and fourth order central finite difference formulas. Following the observation of a high degree of agreement between the exact and current numerical solutions for the Poisson problem, the same difference formulas are used to the Laplace eigenvalue problem, which will be the theme of the subsequent sections.

2.1 Finite Difference Method

The finite difference method is the most well-known and widely used numerical approach for the solution of partial differential equations due to its ease of coding and efficiency in computing. FDM aims to transform the differential equations into difference equations by approximating each derivatives with a difference formula. The finite difference approximations result in algebraic form, and they relate the value of the solution at a point in the computational domain to the values at some nearby points. Thus, the FDM solution procedure implies first discretizing the problem do-

main into a mesh of nodal (grid) points, then approximating the provided differential equation with an equivalent finite difference equation. Finally, the resulting finite difference equations are solved according to the prescribed boundary and/or initial conditions, and the discrete solution is obtained at only the defined grid points in the computational domain. That is, to obtain the solution of a function $u(x, y)$ in a regular rectangular domain $\Omega = [a, b] \times [c, d]$ by using the finite difference scheme, the solution region $\Omega \subset \mathbb{R}^2$ is divided into uniform meshes of sided lengths $\Delta x(= h)$ and $\Delta y(= k)$ as shown in Figure 2.1.

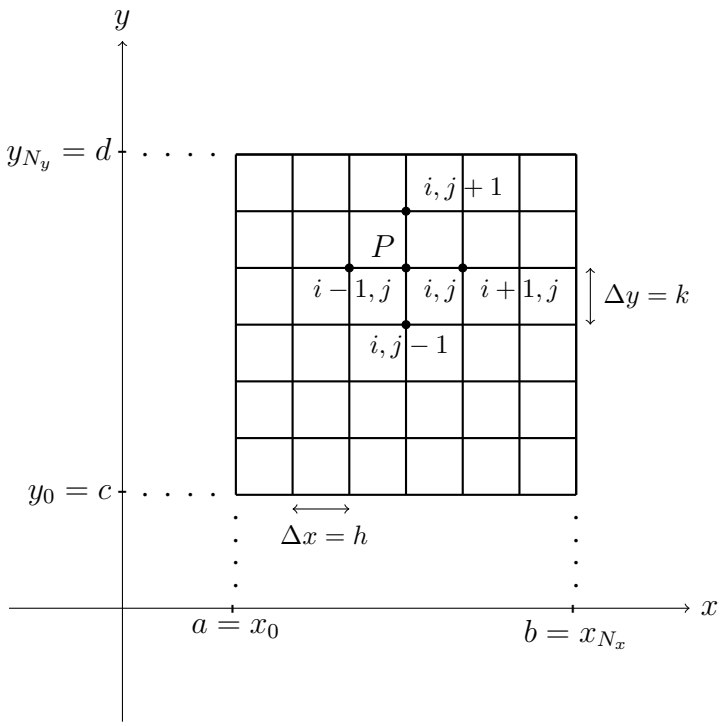

Figure 2.1: The geometry of the meshed rectangular domain Ω.

The components of grid (mesh) point (x, y) are shown by $x_i = a+i\Delta x$, $y_j = c+j\Delta y$ for $i = 0, 1, \cdots, N_x$ and $j = 0, 1, \cdots, N_y$, where N_x and N_y are the number of the subintervals in x and y-directions, respectively. Thus, the step sizes in x-direction becomes $\Delta x = h = \dfrac{b-a}{N_x}$ while $\Delta y = k = \dfrac{d-c}{N_y}$ is in y-direction. The value of u at point $P(x_i, y_j)$ becomes $u(x_i, y_j) = u(a + ih, c + jk) = u_{i,j}$ and the finite difference solution which approximates $u(x_i, y_j)$ is denoted by $U(x_i, y_j) = U_{i,j}$. On the other hand, any approximation of a derivative in differential equations in terms of values at neighboring grid points is called the finite difference approximation. The derivation

of these finite difference formulas for functions of two variables is going to be given by using the well-known Taylor series expansions in x-direction

$$\begin{aligned} u(x_i + \Delta x, y_j) = u(x_i, y_j) &+ \Delta x \frac{\partial u}{\partial x}(x_i, y_j) + \frac{1}{2!}(\Delta x)^2 \frac{\partial^2 u}{\partial x^2}(x_i, y_j) \\ &+ \frac{1}{3!}(\Delta x)^3 \frac{\partial^3 u}{\partial x^3}(x_i, y_j) + \cdots + \frac{1}{(n-1)!}(\Delta x)^{n-1} \frac{\partial^{n-1} u}{\partial x^{n-1}}(x_i, y_j) \\ &+ O(\Delta x^n), \end{aligned} \tag{2.1}$$

$$\begin{aligned} u(x_i - \Delta x, y_j) = u(x_i, y_j) &- \Delta x \frac{\partial u}{\partial x}(x_i, y_j) + \frac{1}{2!}(\Delta x)^2 \frac{\partial^2 u}{\partial x^2}(x_i, y_j) \\ &- \frac{1}{3!}(\Delta x)^3 \frac{\partial^3 u}{\partial x^3}(x_i, y_j) + \cdots + \frac{(-1)^{n-1}}{(n-1)!}(\Delta x)^{n-1} \frac{\partial^{n-1} u}{\partial x^{n-1}}(x_i, y_j) \\ &+ O(\Delta x^n), \end{aligned} \tag{2.2}$$

and similarly, the Taylor series expansions in y-direction

$$\begin{aligned} u(x_i, y_j + \Delta y) = u(x_i, y_j) &+ \Delta y \frac{\partial u}{\partial y}(x_i, y_j) + \frac{1}{2!}(\Delta y)^2 \frac{\partial^2 u}{\partial y^2}(x_i, y_j) \\ &+ \frac{1}{3!}(\Delta y)^3 \frac{\partial^3 u}{\partial y^3}(x_i, y_i) + \cdots + \frac{1}{(n-1)!}(\Delta y)^{n-1} \frac{\partial^{n-1} u}{\partial y^{n-1}}(x_i, y_j) \\ &+ O(\Delta y^n), \end{aligned} \tag{2.3}$$

$$\begin{aligned} u(x_i, y_j - \Delta y) = u(x_i, y_j) &- \Delta y \frac{\partial u}{\partial y}(x_i, y_j) + \frac{1}{2!}(\Delta y)^2 \frac{\partial^2 u}{\partial y^2}(x_i, y_j) \\ &- \frac{1}{3!}(\Delta y)^3 \frac{\partial^3 u}{\partial y^3}(x_i, y_i) + \cdots + \frac{(-1)^{n-1}}{(n-1)!}(\Delta y)^{n-1} \frac{\partial^{n-1} u}{\partial y^{n-1}}(x_i, y_j) \\ &+ O(\Delta y^n), \end{aligned} \tag{2.4}$$

where $O(\Delta x^n)$ and $O(\Delta y^n)$ are the truncation errors arise by truncating the series after the $(n-1)$-st term, in x and y-directions, respectively. We read this error as of order $\Delta x^n (\Delta y^n)$ or $O(\Delta x^n)(O(\Delta y^n))$. Hence, $O(\Delta x^n)$ represents the terms that are having a degree that of not greater than Δx^n. Then, some commonly used finite difference formulas for approximating first and second order derivatives are obtained as follows:

(a) Forward difference formulas for first order partial derivatives: Taylor series expansion of $u(x_i+\Delta x, y_j)$ around (x_i, y_j) given in Equation (2.1) can be written as

$$u(x_i + \Delta x, y_j) = u(x_i, y_j) + \Delta x \frac{\partial u}{\partial x}(x_i, y_j) + O(\Delta x^2). \tag{2.5}$$

Rearranging gives

$$\frac{\partial u}{\partial x}(x_i, y_j) = \frac{u(x_i + \Delta x, y_j) - u(x_i, y_j)}{\Delta x} + O(\Delta x). \tag{2.6}$$

Neglecting the error term $O(\Delta x)$ yields

$$\frac{\partial u}{\partial x}(x_i, y_j) \simeq \frac{u(x_i + \Delta x, y_j) - u(x_i, y_j)}{\Delta x} = \frac{u_{i+1,j} - u_{i,j}}{\Delta x}, \tag{2.7}$$

which is called the forward difference formula for the first order partial derivative of u in x. Similarly, one can obtain the forward difference formula for the first order partial derivative of u with respect to y at the point (x_i, y_j) as:

$$\frac{\partial u}{\partial y}(x_i, y_j) \simeq \frac{u(x_i, y_j + \Delta y) - u(x_i, y_j)}{\Delta y} = \frac{u_{i,j+1} - u_{i,j}}{\Delta y}. \tag{2.8}$$

In these approximations the error is $O(\Delta x)$(or $O(\Delta y)$), so they are called the first order approximations.

(b) Backward difference formulas for first order partial derivatives: Once Equation (2.2) and Equation (2.4) are rearranged leaving the terms $\partial u/\partial x$ and $\partial u/\partial y$ alone on the right hand side, we have

$$\frac{\partial u}{\partial x}(x_i, y_j) = \frac{u(x_i, y_j) - u(x_i - \Delta x, y_j)}{\Delta x} + O(\Delta x), \tag{2.9}$$

and

$$\frac{\partial u}{\partial y}(x_i, y_j) = \frac{u(x_i, y_j) - u(x_i, y_j - \Delta y)}{\Delta y} + O(\Delta y), \tag{2.10}$$

which yield the first order backward finite difference formulas to approximate $\partial u/\partial x$ and $\partial u/\partial y$ given as follows:

$$\left.\frac{\partial u}{\partial x}\right|_{i,j} \simeq \frac{u_{i,j} - u_{i-1,j}}{\Delta x}, \tag{2.11}$$

and

$$\left.\frac{\partial u}{\partial y}\right|_{i,j} \simeq \frac{u_{i,j} - u_{i,j-1}}{\Delta y}. \tag{2.12}$$

(c) Central difference formulas for first order partial derivatives: By subtracting the expansion (2.2) from the expansion (2.1) and rearranging, the partial derivative of u with respect to x becomes

$$\frac{\partial u}{\partial x}(x_i, y_j) = \frac{u(x_i + \Delta x, y_j) - u(x_i - \Delta x, y_j)}{2\Delta x} + O(\Delta x^2), \tag{2.13}$$

which yields the central difference approximation

$$\left.\frac{\partial u}{\partial x}\right|_{i,j} \simeq \frac{u_{i+1,j} - u_{i-1,j}}{2\Delta x}. \tag{2.14}$$

Similarly, the central difference formula for $\dfrac{\partial u}{\partial y}$ at (x_i, y_j) is:

$$\left.\frac{\partial u}{\partial y}\right|_{i,j} \simeq \frac{u_{i,j+1} - u_{i,j-1}}{2\Delta y}. \tag{2.15}$$

Here, the error term is of order Δx^2(or Δy^2), so the central difference formulas are second order approximations.

(d) Central difference formulas for second order partial derivatives: By adding the expansions (2.1) and (2.2), we obtain

$$u(x_i + \Delta x, y_j) + u(x_i - \Delta x, y_j) = 2u(x_i, y_j) + (\Delta x)^2 \frac{\partial^2 u}{\partial x^2}(x_i, y_j) + O(\Delta x^4), \tag{2.16}$$

which can be written as

$$\frac{\partial^2 u}{\partial x^2}(x_i, y_j) = \frac{u(x_i + \Delta x, y_j) - 2u(x_i, y_j) + u(x_i - \Delta x, y_j)}{\Delta x^2} + O(\Delta x^2). \tag{2.17}$$

Neglecting the error term, one can obtain the so called central difference formula for $\dfrac{\partial^2 u}{\partial x^2}$ of second order as:

$$\left.\frac{\partial^2 u}{\partial x^2}\right|_{i,j} \simeq \frac{u_{i+1,j} - 2u_{i,j} + u_{i-1,j}}{\Delta x^2}. \tag{2.18}$$

On the other hand, adding expansions (2.3) and (2.4) the second order central difference formula for $\dfrac{\partial^2 u}{\partial y^2}$ at (x_i, y_j) is obtained as:

$$\left.\frac{\partial^2 u}{\partial y^2}\right|_{i,j} \simeq \frac{u_{i,j+1} - 2u_{i,j} + u_{i,j-1}}{\Delta y^2}. \tag{2.19}$$

Higher order finite difference formulas approximating the partial derivatives can be derived by taking more terms in Taylor series expansions and combining these expansions around different points. For example, the fourth order central difference formula to approximate the first and second order partial derivatives with respect to x:

$$\left.\frac{\partial u}{\partial x}\right|_{i,j} = \frac{-u_{i+2,j} + 8u_{i+1,j} - 8u_{i-1,j} + u_{i-2,j}}{12\Delta x} + O(\Delta x^4) \tag{2.20}$$

and

$$\left.\frac{\partial^2 u}{\partial x^2}\right|_{i,j} = \frac{-u_{i+2,j} + 16u_{i+1,j} - 30u_{i,j} + 16u_{i-1,j} - u_{i-2,j}}{12\Delta x^2} + O(\Delta x^4) \tag{2.21}$$

are obtained by combining the Taylor series expansions of u at the points $(x_i - 2\Delta x, y_j)$, $(x_i - \Delta x, y_j)$, $(x_i + \Delta x, y_j)$ and $(x_i + 2\Delta x, y_j)$ about (x_i, y_j). Similarly, the corresponding fourth order central difference formulas for the first and second order derivatives with respect to y are obtained by combining the Taylor series expansions of u at the points $(x_i, y_j - 2\Delta y)$, $(x_i, y_j - \Delta y)$, $(x_i, y_j + \Delta y)$ and $(x_i, y_j + 2\Delta y)$ about (x_i, y_j) as follows:

$$\left.\frac{\partial u}{\partial y}\right|_{i,j} = \frac{-u_{i,j+2} + 8u_{i,j+1} - 8u_{i,j-1} + u_{i,j-2}}{12\Delta y} + O(\Delta y^4) \tag{2.22}$$

and

$$\left.\frac{\partial^2 u}{\partial y^2}\right|_{i,j} = \frac{-u_{i,j+2} + 16u_{i,j+1} - 30u_{i,j} + 16u_{i,j-1} - u_{i,j-2}}{12\Delta y^2} + O(\Delta y^4). \tag{2.23}$$

2.2 Application of the FDM and Numerical Results

The present section is devoted to give the application of the FDM to the basic elliptic type partial differential equations in a detailed way, namely for the Poisson problem and the Laplace eigenvalue problem defined in a square domain. The second and fourth order central difference formulas given in Section 2.1 are used for the discretization of the Laplace operator in these equations.

2.2.a Test Problem 1: Poisson Problem

The two-dimensional Poisson equation is a well-known elliptic partial differential equation that has the following related form when supplied with mixed type boundary

conditions:

$$\begin{cases} -\Delta u = f(x,y) & \text{in } \Omega, \\ \alpha u + \beta \dfrac{\partial u}{\partial n} = g(x,y) & \text{on } \partial\Omega, \end{cases} \tag{2.24}$$

where $\Delta = \partial^2/\partial x^2 + \partial^2/\partial y^2$ is the Laplacian operator, $u(x,y)$ is some scalar potential which will be determined, $f(x,y)$ is a known source function, and Ω is the domain of the solution with boundary $\partial\Omega$. In the mixed type boundary condition, α, β are constants and $g(x,y)$ is a given function. The Poisson problem describes generally a variety of potential-related events concerned with physical potentials such as thermodynamic or electrostatic potentials. The determination of the electrical potential for a given charge distribution and the calculation of the gravitational force can be given as the sample applications of the Poisson problem [43, 44].

A finite difference scheme for the solution of Poisson problem (2.24) is obtained by first discretizing the domain, which is taken as a rectangular region $\Omega = [a,b] \times [c,d]$, and then discretizing the Poisson equation by replacing the derivatives with the appropriate finite difference formulas given in Section 2.1. Once the domain is discretized with a uniform mesh by taking N_x and N_y equal length subintervals, respectively in x and y-directions, this yields the corresponding mesh sizes $\Delta x = h = (b-a)/N_x$ and $\Delta y = k = (d-c)/N_y$. Hence, a mesh Ω_h on Ω becomes

$$\begin{aligned} \Omega_h = \{(x_i, y_j) :\ & x_i = a + (i-1)h,\ i = 1, \ldots, N_x + 1, \\ & y_j = c + (j-1)k,\ j = 1, \ldots, N_y + 1\} \end{aligned}$$

where (x_i, y_j) are the mesh points. Then, the Laplace operator in Poisson equation (2.24) at an interior node (x_i, y_j) can be approximated by using finite difference formulas of different orders. The boundary conditions are also approximated by using a suitable finite difference formula for the first order derivatives. This results in a system of linear algebraic equations

$$AU = z, \tag{2.25}$$

where A is a well-structured sparse matrix by using a suitable choice of ordering in the solution vector U involving the unknown values of u both in the interior and on the boundary of the problem depending on the type of the boundary conditions.

In order to validate our finite difference computer codes in MATLAB, the numerical simulations are performed to approximate the solution of the Poisson problem

$$\begin{cases} -\Delta u = \sin(x)\sin(y) & \text{in } \Omega, \\ u = 0 & \text{on } \partial\Omega, \end{cases} \tag{2.26}$$

in a square domain $\Omega = \{(x, y) : 0 \leq x, y \leq \pi\}$, for which the analytical solution is

$$u(x, y) = \frac{1}{2}\sin(x)\sin(y)\,. \tag{2.27}$$

The discrete solution is obtained by using FDM of different orders. That is, the second order central difference formulas (2.18)-(2.19) and fourth order central difference formulas (2.21)-(2.23) are going to be employed in Section 2.2.a.1 and Section 2.2.a.2, respectively, to approximate the partial derivatives u_{xx} and u_{yy} in the Laplace operator.

2.2.a.1 Approximation of the Poisson Equation by Second Order Finite Central Difference Formulas

In this section, the derivatives u_{xx} and u_{yy} in the Laplace operator are replaced by the second order central difference formulas (2.18)-(2.19) at an interior node (x_i, y_j). Thus, Equation (2.26) at (x_i, y_j) becomes

$$-\frac{U_{i+1,j} - 2U_{i,j} + U_{i-1,j}}{h^2} - \frac{U_{i,j+1} - 2U_{i,j} + U_{i,j-1}}{k^2} = \sin(x_i)\sin(y_j), \tag{2.28}$$

where $U_{i,j}$ is an approximation of $u(x_i, y_j)$, $1 \leq i \leq N_x$, $1 \leq j \leq N_y$, $h = \pi/N_x$, $k = \pi/N_y$, and $x_i = i\pi/N_x,\ y_j = j\pi/N_y$. When, $h = k$, Equation (2.28) is simplified to

$$4U_{i,j} - U_{i+1,j} - U_{i-1,j} - U_{i,j+1} - U_{i,j-1} = \frac{\pi^2}{N^2}\sin(i\frac{\pi}{N})\sin(j\frac{\pi}{N}), \tag{2.29}$$

which is the so-called five point finite difference formula for $i, j = 1, 2, \ldots, N$ with $N = N_x = N_y$. The corresponding discretized boundary conditions are obtained as

$$\begin{aligned} u(1, y) = U_{N,j} = 0, \quad u(x, 0) = U_{i,0} = 0, \\ u(0, y) = U_{0,j} = 0, \quad u(x, 1) = U_{i,N} = 0\,. \end{aligned} \tag{2.30}$$

After the insertion of boundary conditions into the difference equation (2.29), one can obtain the system of linear equations in the matrix-vector form as follows:

$$AU = \left(\frac{\pi}{N}\right)^2 z, \tag{2.31}$$

when the unknown vector U is ordered in the following form:

$$U^T = \Big[U_{1,1} \quad U_{2,1} \quad \cdots \quad U_{N-1,1} \quad | \quad U_{1,2} \quad U_{2,2} \quad \cdots \quad U_{N-1,2} \quad | \quad \cdots \quad | \quad U_{1,N-1} \quad U_{2,N-1} \quad \cdots \quad U_{N-1,N-1}\Big]. \quad (2.32)$$

Here, the coefficient matrix A of size $(N-1)^2 \times (N-1)^2$ is a sparse block tridiagonal matrix constructed by the matrix D and the identity matrix I of size $(N-1)\times(N-1)$:

$$A = \begin{bmatrix} D & -I & 0 & \cdots & \cdots & 0 \\ -I & D & -I & \ddots & & \vdots \\ 0 & -I & D & \ddots & \ddots & \vdots \\ \vdots & \ddots & \ddots & \ddots & 0 & \vdots \\ \vdots & & \ddots & 0 & -I & \vdots \\ 0 & \cdots & \cdots & 0 & -I & D \end{bmatrix}, \quad D = \begin{bmatrix} 4 & -1 & 0 & \cdots & \cdots & 0 \\ -1 & 4 & -1 & \ddots & & \vdots \\ 0 & -1 & 4 & \ddots & \ddots & \vdots \\ \vdots & \ddots & \ddots & \ddots & 0 & \vdots \\ \vdots & & \ddots & 0 & -1 & \vdots \\ 0 & \cdots & \cdots & 0 & -1 & 4 \end{bmatrix}.$$

The right hand side vector z is

$$z^T = \Big[f_1 g_1 \quad f_2 g_1 \quad \cdots \quad f_{N-1} g_1 \quad | \quad f_1 g_2 \quad f_2 g_2 \quad \cdots \quad f_{N-1} g_2 \quad | \quad \cdots \quad | \quad f_1 g_{N-1} \quad f_2 g_{N-1} \quad \cdots \quad f_{N-1} g_{N-1}\Big], \quad (2.33)$$

where $f_i = \sin(x_i)$ and $g_j = \sin(y_j)$.

In Figure 2.2, a qualitative comparison between the analytical and FDM solution with the second order central difference formulas is visualized in terms of contour plots. It is observed that the numerical solution matches very well with the exact solution.

On the other hand, as the number of mesh points N increases, or equivalently as the uniform mesh size $h = \pi/N$ decreases, the convergence behavior of the FDM solution to the exact solution is examined. The relative error $\varepsilon = \frac{\|u-U\|_2}{\|u\|_2}$ (with respect to L^2-norm, $\|u\|_2 = \sqrt{{u_1}^2 + {u_2}^2 + \cdots + {u_n}^2}$ where $u = (u_1, u_2, \cdots, u_n)$) between the exact solution u and the approximate solution U is plotted on a log-log scale in Figure 2.3 for $N = 8, 16, \cdots, 4096$ to show this convergence behavior. The line with asterisks represents the change in the error for decreasing values of h and the blue line shows just a line with slope $m = -2$. As seen in Figure 2.3, the convergence behavior of the approximate solution U is of order $O(h^2)$ as expected by the use of second order central difference formulas to approximate derivatives.

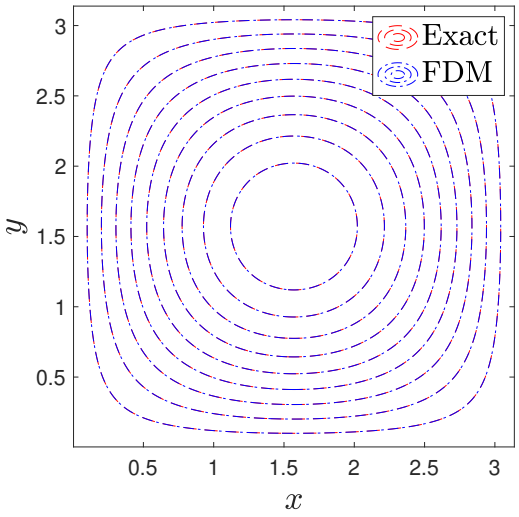

Figure 2.2: Exact and approximate solutions of Poisson problem by second order difference formula.

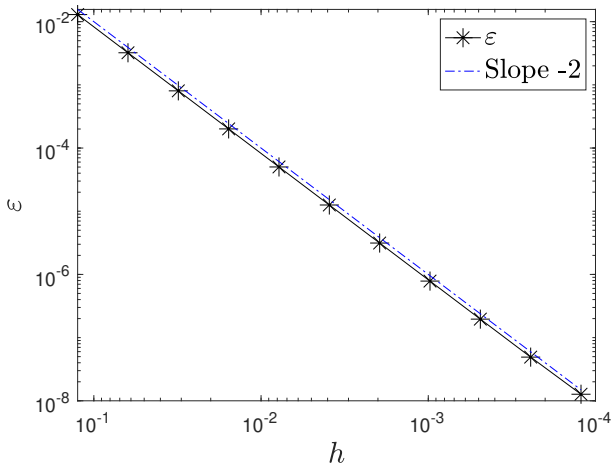

Figure 2.3: Convergence rate of $O(h^2)$ for the Poisson problem by second order difference formula.

2.2.a.2 Approximation of the Poisson Equation by Fourth Order Central Difference Formulas

In the discretization of the Poisson equation (2.26), the fourth order central difference formulas (2.21)-(2.23) are applied at point (x_i, y_j) by taking same number of equally spaced mesh points N in x and y-directions, that is $h = k$, as in the previous section. This results in the following finite difference equation

$$-\frac{1}{12h^2}(-U_{i+2,j} + 16U_{i+1,j} - 30U_{i,j} + 16U_{i-1,j} - U_{i-2,j}) - \frac{1}{12h^2}(-U_{i,j+2} + 16U_{i,j+1} - 30U_{i,j} + 16U_{i,j-1} - U_{i,j-2}) = \sin(x_i)\sin(y_j), \tag{2.34}$$

which can be rewritten as:

$$\begin{aligned} -U_{i+2,j} + 16U_{i+1,j} - 60U_{i,j} + 16U_{i-1,j} - U_{i-2,j} - U_{i,j+2} + 16U_{i,j+2} + 16U_{i,j-1} \\ -U_{i,j-2} = -12h^2 \sin(i\frac{\pi}{N}) \sin(j\frac{\pi}{N}), \end{aligned} \tag{2.35}$$

for $i, j = 1, 2, \cdots, N-1$. The discretized form of the homogeneous boundary conditions are

$$\begin{aligned} u(1,y) = U_{N,j} = 0, \quad u(x,0) = U_{i,0} = 0, \\ u(0,y) = U_{0,j} = 0, \quad u(x,1) = U_{i,N} = 0\,. \end{aligned} \tag{2.36}$$

When the difference equation is written for the values of $i, j = 1, 2, \cdots, N-1$, some fictitious points, the points which are not in the computational domain, appear in the system of equations. Thus, for the evaluation of the unknown values only in the computational domain Ω_h, the values of the unknown U at these ghost points are required, and in the computations these values are obtained from the exact solution as follows:

$$\begin{aligned} U_{i,-1} = \frac{1}{2}\sin(\frac{i\pi}{N})\sin(-\frac{\pi}{N}), \quad U_{i,N+1} = \frac{1}{2}\sin(\frac{i\pi}{N})\sin(\frac{(N+1)\pi}{N}), \\ U_{-1,j} = \frac{1}{2}\sin(-\frac{\pi}{N})\sin(\frac{j\pi}{N}), \quad U_{N+1,j} = \frac{1}{2}\sin(\frac{(N+1)\pi}{N})\sin(\frac{j\pi}{N})\,. \end{aligned} \tag{2.37}$$

The use of exact values at this stage is due to the fact that we aim to test our algorithms using these forms. Nevertheless, these boundary conditions can be approximated by other means. After the insertion of the related ghost points and the boundary conditions, and with a suitable ordering of the unknown values

$$\begin{aligned} U^T = \Big[U_{1,1} \;\; U_{2,1} \;\; \cdots \;\; U_{N-1,1} \;\; | \;\; U_{1,2} \;\; U_{2,2} \;\; \cdots \;\; U_{N-1,2} \;\; | \;\; \cdots \\ | \;\; U_{1,N-1} \;\; U_{2,N-1} \;\; \cdots \;\; U_{N-1,N-1} \Big], \end{aligned} \tag{2.38}$$

one can obtain the following system of linear equations in matrix-vector form:

$$AU = z, \tag{2.39}$$

where the coefficient matrix A of size $(N-1)^2 \times (N-1)^2$ is the block tridiagonal matrix. It is formed by the identity matrix I and the matrix D of size $(N-1)\times(N-1)$

and given as:

$$A = \begin{bmatrix} D & 16I & -I & 0 & \cdots & & & & 0 \\ 16I & D & 16I & -I & & & & & \\ -I & 16I & D & 16I & -I & & & & \\ 0 & -I & 16I & D & 16I & & & & \\ \vdots & & & & & & & & 0 \\ & & & & & & D & 16I & -I \\ & & & & & 0 & -I & 16I & D & 16I \\ 0 & \cdots & & & & 0 & 0 & -I & 16I & D \end{bmatrix},$$

$$D = \begin{bmatrix} -60 & 16 & -1 & 0 & \cdots & & & & 0 \\ 16 & -60 & 16 & -1 & & & & & \\ -1 & 16 & -60 & 16 & -1 & & & & \\ 0 & -1 & 16 & -60 & 16 & & & & \\ \vdots & & & & & & & & 0 \\ & & & & & & -60 & 16 & -1 \\ & & & & & 0 & -1 & 16 & -60 & 16 \\ 0 & \cdots & & & & 0 & 0 & -1 & 16 & -60 \end{bmatrix}.$$

Using spy code in MATLAB, the coefficient matrix A for $N = 10$ is presented in Figure 2.4. The non-zero entries of the matrix A are represented by the dots in the figure.

The vector z is the linear combination of the vectors formed by the functions $f_i = \sin(x_i)$, $g_j = \sin(y_j)$, that is:

$$z = -12h^2 r + \frac{s}{2} + \frac{t}{2}, \tag{2.40}$$

where

$$r^T = \Big[| f_1 g_1 \quad f_2 g_1 \quad \cdots \quad f_{N-1} g_1 \quad | \quad f_1 g_2 \quad f_2 g_2 \quad \cdots \quad f_{N-1} g_2 \quad | \quad \cdots \quad | \quad f_1 g_{N-1} \quad f_2 g_{N-1} \quad \cdots \quad f_{N-1} g_{N-1} \Big], \tag{2.41}$$

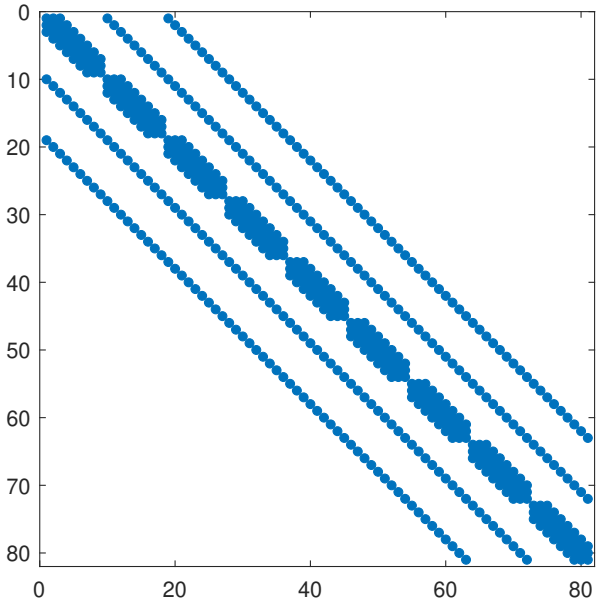

Figure 2.4: Sparsity pattern of the coefficient matrix A when $N = 10$.

$$s^T = \Big[f_1 g_{-1} \quad f_2 g_{-1} \quad \cdots \quad f_{N-1} g_{-1} \quad | \quad 0 \quad \cdots \quad 0 \quad | \quad f_1 g_{N+1} \quad f_2 g_{N+1} \quad \cdots \quad f_{N-1} g_{N+1} \Big], \tag{2.42}$$

$$t^T = \Big[f_{-1} g_1 \quad 0 \quad \cdots \quad 0 \quad f_{N+1} g_1 \quad | \quad f_{-1} g_2 \quad 0 \quad \cdots \quad 0 \quad f_{N+1} g_2 \quad | \quad \cdots \quad | \quad f_{-1} g_{N-1} \quad 0 \quad \cdots \quad 0 \quad f_{N+1} g_{N-1} \Big]. \tag{2.43}$$

Figure 2.5 displays the well agreement of the exact and FDM solutions of the Poisson problem in terms of level surfaces. The relative error between the approximate solution obtained using the fourth order central difference formulas and the exact solution is drawn in log-log scale in Figure 2.6 to visualize the convergence behavior of the FDM solution to the exact solution regarding the values of $h = \pi/N$ with $N = 8, 16, \cdots, 2048$. A fourth order $O(h^4)$ rate of convergence is well observed from Figure 2.6.

To summarize, the Poisson problem is solved using the finite difference approach with the second and fourth order central difference formulas for the approximation of the Laplace operator. Despite the fact that both difference formulas produce precise

(a) FDM Solution **(b)** Exact Solution

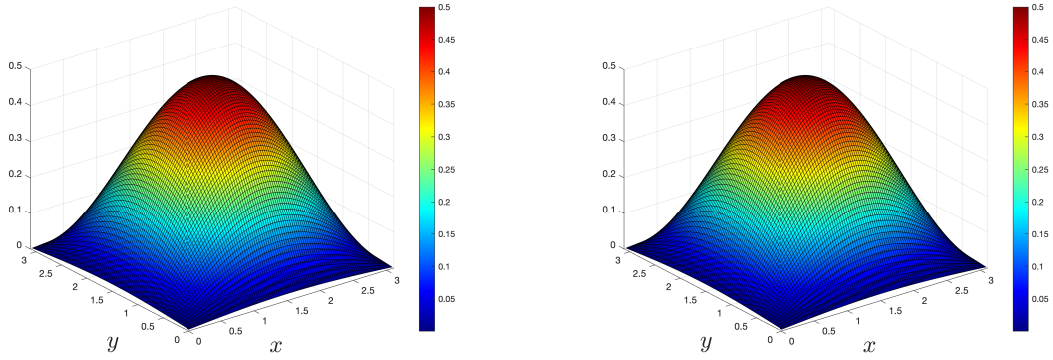

Figure 2.5: FDM and exact solutions of Poisson problem by fourth order difference formula.

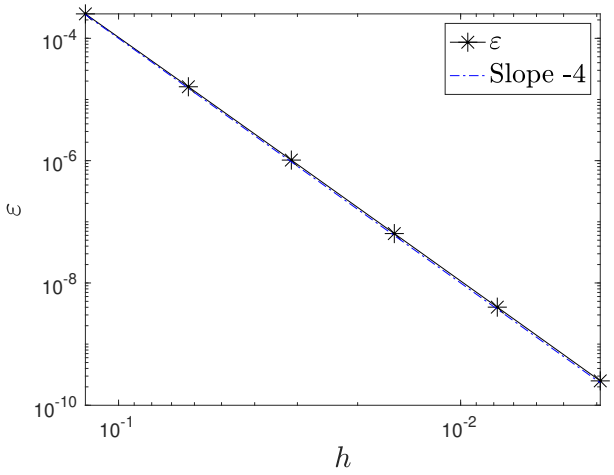

Figure 2.6: Convergence rate of $O(h^4)$ for the Poisson problem by fourth order difference formula.

results, the convergence of the approximate solution to the exact solution is faster in the fourth order scheme. That is, in the second order scheme the convergence behavior of the FDM solution is of order $O(h^2)$ whereas in fourth order scheme, it is of order $O(h^4)$.

2.2.b Test Problem 2: The Laplace Eigenvalue Problem

The two-dimensional eigenvalue problem for the Laplacian is investigated on a bounded domain $\Omega \subset \mathbb{R}^2$. Specifically, we search pairs (λ, u) where $\lambda \in \mathbb{R}$ is called an eigenvalue of the Laplacian and function $u \neq 0$ is the corresponding eigenfunction in Ω.

Thus, the Laplace eigenvalue problem is defined as:

$$\begin{cases} -\Delta u = \lambda u & \text{in } \Omega, \\ u = 0 & \text{on } \partial\Omega, \end{cases} \tag{2.44}$$

for which λ and u form the eigensolution.

It is well-known that one can obtain the analytical solution of the Laplace EVP in a square $[0, L] \times [0, L]$ by using the method of separation of variables. Then, the Laplace EVP for this domain can be written explicitly as:

$$-u_{xx} - u_{yy} = \lambda u, \tag{2.45}$$

$$u(0, y) = 0, \tag{2.46}$$

$$u(L, y) = 0, \tag{2.47}$$

$$u(x, 0) = 0, \tag{2.48}$$

$$u(x, L) = 0. \tag{2.49}$$

Suppose that the solution is written in the form

$$u(x, y) = X(x)Y(y), \tag{2.50}$$

and then the partial derivatives become

$$u_{xx} = X''Y,\ u_{yy} = XY''. \tag{2.51}$$

Inserting these partials in Equation (2.45), and dividing by XY (assuming $XY \neq 0$ since $u \neq 0$) we obtain

$$-\frac{X''}{X} - \frac{Y''}{Y} = \lambda. \tag{2.52}$$

If it is assumed that $\lambda = a + b$ such that $a = -\dfrac{X''}{X}$ and $b = -\dfrac{Y''}{Y}$, two ordinary differential equations with the boundary conditions are obtained as

$$X'' + aX = 0, \tag{2.53}$$

$$Y'' + bY = 0, \tag{2.54}$$

with the boundary conditions $X(0) = X(L) = 0$ obtained from Equations (2.46) and (2.47) for Equation (2.53), and $Y(0) = Y(L) = 0$ using Equations (2.48) and (2.49) for Equation (2.54).

When $a \leq 0$, the ODE in Equation (2.53) with the given boundary conditions has

trivial solution $X = 0$ which gives $u(x, y) = X(x)Y(y) = 0$. In fact, if it is assumed that $a < 0$, the general solution of (2.53), using roots $r_{1,2} = \pm\sqrt{a}$ of its characteristic polynomial $r^2 + a = 0$, is

$$X(x) = c_1 e^{\sqrt{a}x} + c_2 e^{-\sqrt{a}x}, \tag{2.55}$$

where c_1 and c_2 are some constants. The only solution that satisfies the boundary conditions is $X = 0$. In case of $a = 0$ the general solution of Equation (2.53) is $X(x) = c_1 x + c_2$, and the trivial solution $X = 0$ is obtained when the boundary conditions are applied. Similarly, the trivial solution $Y = 0$ can be obtained for Equation (2.54) where $b \leq 0$ in the given boundary conditions. On the other hand, when $a > 0$ and $b > 0$, the solutions of Equations (2.53) and (2.54) can be written as

$$X(x) = c_1 \sin(\sqrt{a}x) + c_2 \cos(\sqrt{a}x), \tag{2.56}$$

$$Y(y) = c_3 \sin(\sqrt{b}y) + c_4 \cos(\sqrt{b}y), \tag{2.57}$$

where c_1, c_2, c_3 and c_4 are arbitrary constants. From the conditions (2.46) and (2.48), it is obtained that $c_2 = c_4 = 0$. On the other hand, applying the conditions (2.47) and (2.49) yields

$$c_1 \sin(\sqrt{a}x) = 0, \tag{2.58}$$

$$c_3 \sin(\sqrt{b}y) = 0. \tag{2.59}$$

Using the boundary conditions $X(L) = 0$ and $Y(L) = 0$ results in

$$c_1 \sin(\sqrt{a}L) = 0, \tag{2.60}$$

$$c_3 \sin(\sqrt{b}L) = 0, \tag{2.61}$$

respectively. For a nontrivial solution, we must have $\sqrt{a}L = m\pi$ and $\sqrt{b}L = n\pi$ for some positive integers m and n. Finally, the solution for the eigenvalues are

$$\lambda_{m,n} = a + b = \left(\frac{m\pi}{L}\right)^2 + \left(\frac{n\pi}{L}\right)^2, \text{ where } m, n \in \mathbb{Z}^+, \tag{2.62}$$

with the corresponding non-zero eigenfunctions

$$u^{m,n} = c \sin\left(\frac{m\pi x}{L}\right) \sin\left(\frac{n\pi y}{L}\right), \ c \in \mathbb{R}. \tag{2.63}$$

On the other hand, in numerical simulations by using second and fourth order finite difference scheme, we consider the eigenvalue problem on the unit square $\Omega = [0,1] \times [0,1]$ that is:

$$\begin{cases} -\Delta u = -u_{xx} - u_{yy} = \lambda u & \text{in } \Omega, \\ u(1,y) = u(0,y) = u(x,0) = u(x,1) = 0 & \text{on } \partial\Omega, \end{cases} \tag{2.64}$$

and the exact solution is

$$u^{m,n} = \sin(m\pi x)\sin(n\pi y), \quad \lambda_{m,n} = (m\pi)^2 + (n\pi)^2, \ m,n \in \mathbb{Z}^+. \tag{2.65}$$

The computational domain is discretized by using a uniform mesh with grid points $(x_i = ih, y_j = jh)$, $0 \leq i,j \leq N$ and $h = 1/N$ with N being the number of subintervals in x and y-directions.

2.2.b.1 Approximation of the Laplace EVP by Second Order Central Difference Formulas

When the partial derivatives u_{xx} and u_{yy} in Equation (2.64) are approximated by the second order central difference formulas (2.18) and (2.19), we obtain the discrete eigenvalue problem

$$\frac{4U_{i,j} - U_{i+1,j} - U_{i-1,j} - U_{i,j+1} - U_{i,j-1}}{h^2} = \lambda U_{i,j}, \tag{2.66}$$

for $i,j = 1,2,\ldots,N-1$ with the boundary conditions

$$\begin{aligned} u(1,y) = U_{N,j} = 0, \quad u(x,0) = U_{i,0} = 0, \\ u(0,y) = U_{0,j} = 0, \quad u(x,1) = U_{i,N} = 0\,. \end{aligned} \tag{2.67}$$

The difference equation (2.66) for $1 \leq i,j \leq N-1$ yields $(N-1)^2$ linear equations which can be written in the matrix form

$$AU = \tilde{\lambda} U, \tag{2.68}$$

which is a matrix eigenvalue problem with $\tilde{\lambda} = \lambda/N^2$. Here U is the reduced vector after the insertion of homogeneous boundary conditions and is taken in the following ordering

$$\begin{aligned} u^T = \Big[U_{1,1} \ \ U_{2,1} \ \ \cdots \ \ U_{N-1,1} \ \ | \ \ U_{1,2} \ \ U_{2,2} \ \ \cdots \ \ U_{N-1,2} \ \ | \ \ \cdots \\ | \ \ U_{1,N-1} \ \ U_{2,N-1} \ \ \cdots \ \ U_{N-1,N-1} \Big]\,. \end{aligned} \tag{2.69}$$

Then the matrix A has the form

$$A = \begin{bmatrix} D & -I & 0 & \cdots & 0 \\ -I & D & -I & & \\ 0 & -I & D & & \\ \vdots & & & 0 & \\ & & & -I & \\ 0 & \cdots & 0 & -I & D \end{bmatrix} \text{,where} \quad D = \begin{bmatrix} 4 & -1 & 0 & \cdots & 0 \\ -1 & 4 & -1 & & \\ 0 & -1 & 4 & & \\ \vdots & & & 0 & \\ & & & -1 & \\ 0 & \cdots & 0 & -1 & 4 \end{bmatrix},$$

and I is the identity matrix of size $(N-1) \times (N-1)$ as the matrices obtained in Section 2.2.a.1 for the Poisson problem. Since A is a sparse matrix, the eigenvalue solvers for sparse matrices are employed in our MATLAB code. Once the system (2.68) is solved, the discrete eigensolutions $(\lambda_{m,n}^h, U)$ are obtained.

In Table 2.1, we present the smallest ten approximate eigenvalues $\lambda_{m,n}^h$ and exact eigenvalues $\lambda_{m,n}$ of the Laplace EVP for $N = 100, 500, \cdots, 3000$. In the last column for $N = 3000$, the normalized errors $\varepsilon_{m,n} = \left| \dfrac{\lambda_{m,n} - \lambda_{m,n}^h}{\lambda_{m,n}} \right|$ are also given for each eigenvalue. It is seen from Table 2.1 that as the number of grid points N increases, the approximate eigenvalues $\lambda_{m,n}^h$ approach the exact eigenvalues $\lambda_{m,n}$ with an error of less than 10^{-5}. Moreover, the smaller eigenvalues are better approximated than bigger ones especially for small N. Indeed, the relative error is much smaller for the smaller eigenvalues than the ones corresponding to the larger ones.

Table 2.1: First ten ordered eigenvalues of the Laplace EVP by second order difference formula.

(m,n)	$\lambda_{m,n}$	$N = 100$	$N = 500$	$N = 1000$	$N = 2000$	$N = 3000$ ($\varepsilon_{m,n}$)
$(1,1)$	19.7392	19.7376	19.7391	19.7392	19.7392	19.7392(9.00e-07)
$(1,2)$	49.3480	49.3342	49.3475	49.3479	49.3480	49.3480(3.10e-06)
$(2,1)$	49.3480	49.3342	49.3475	49.3479	49.3480	49.3480(3.10e-06)
$(2,2)$	78.9568	78.9309	78.9558	78.9566	78.9568	78.9568(3.70e-06)
$(1,3)$	98.6960	98.6295	98.6934	98.6954	98.6959	98.6960(7.50e-06)
$(3,1)$	98.6960	98.6295	98.6934	98.6954	98.6959	98.6960(7.50e-06)
$(2,3)$	128.3049	128.2261	128.3017	128.3041	128.3047	128.3048(6.80e-06)
$(3,2)$	128.3049	128.2261	128.3017	128.3041	128.3047	128.3048(6.80e-06)
$(1,4)$	167.7833	167.5748	167.7749	167.7812	167.7828	167.7830(1.38e-05)
$(4,1)$	167.7833	167.5748	167.7749	167.7812	167.7828	167.7830(1.38e-05)

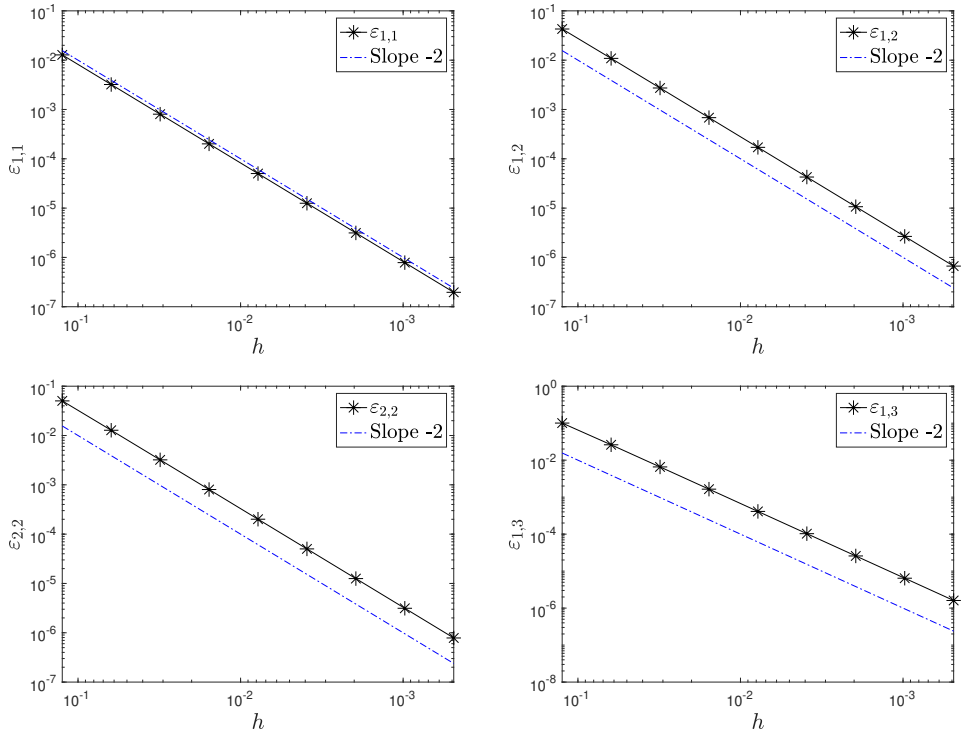

Figure 2.7: Convergence behavior of $\lambda_{m,n}^h$ to $\lambda_{m,n}$ versus the step size h in log-log scale by second order difference formula.

To illustrate the convergence behaviour of the approximate eigenvalues $\lambda_{m,n}^h$ to the exact ones, the normalized errors $\varepsilon_{m,n}$ are plotted in Figure 2.7 for the first five eigenvalues, and it is observed that approximate eigenvalues converges to exact ones with an order of $O(h^2)$. Since the eigenvalues $\lambda_{1,2}$ and $\lambda_{2,1}$ are the same, only the convergence behavior for $\lambda_{1,2}$ is presented.

2.2.b.2 Approximation of the Laplace EVP by Fourth Order Difference Formulas

Although the FDM is easy to implement, some difficulties arise in imposing the boundary conditions when higher order finite difference formulas requiring ghost points, are applied. In the Poisson problem by the fourth order finite differences in Section 2.2.a.2, the value at the ghost points are found by using the exact solutions, however, in Laplace EVP a different fourth order FDM, described in [45], is employed for the discretization of the Laplace eigenvalue differential equation. This new finite difference scheme is called compact finite difference (FD) scheme, in which the

coefficients are computed by a formulation of Taylor expansion with symmetric polynomials. The aim of the compact finite difference scheme is to increase the accuracy of FDM on Cartesian grids with mesh size $h > 0$, without increasing the size of the associated stencil. The fourth order compact scheme in two-dimensions for the Poisson equation $-\Delta u = f$ is given as [45],

$$\frac{1}{6h^2}(-U_{i-1,j-1} - 4U_{i,j-1} - U_{i+1,j-1} - 4U_{i-1,j} + 20U_{i,j} - 4U_{i+1,j} - U_{i-1,j+1} \\ -4U_{i,j+1} - U_{i+1,j+1}) = \frac{1}{12}(f_{i+1,j} + 8f_{i,j} + f_{i-1,j} + f_{i,j+1} + f_{i,j-1}), \tag{2.70}$$

for which the truncation error is of order $O(h^4)$ and is equal to

$$TE = -\frac{h^4}{90}\left[\frac{\partial^6 u}{\partial x^6} + \frac{\partial^6 u}{\partial y^6}\right] + O(h^5), \tag{2.71}$$

when a uniform mesh with $h = k = 1/N$ is used. Thus, the compact FD equation for the Laplace EVP can be obtained as:

$$\frac{1}{6h^2}(-U_{i-1,j-1} - 4U_{i,j-1} - U_{i+1,j-1} - 4U_{i-1,j} + 20U_{i,j} - 4U_{i+1,j} - U_{i-1,j+1} \\ -4U_{i,j+1} - U_{i+1,j+1}) = \frac{\lambda}{12}(U_{i+1,j} + 8U_{i,j} + U_{i-1,j} + U_{i,j+1} + U_{i,j-1}), \tag{2.72}$$

by taking the RHS function in Equation (2.70) as $f = \lambda u$ for $i, j = 1, 2, \ldots, N-1$ with the same boundary conditions given in Equation (2.67). The difference Equation (2.72) for $1 \leq i, j \leq N-1$ produces $(N-1)^2$ linear equations that can be written as:

$$T_1 U = \tilde{\lambda} T_2 U, \tag{2.73}$$

which is a generalized eigenvalue problem with $\tilde{\lambda} = 6h^2\lambda/12$. Here,

$$u^T = \Big[u_{1,1} \quad u_{2,1} \quad \cdots \quad u_{N-1,1} \quad | \quad u_{1,2} \quad u_{2,2} \quad \cdots \quad u_{N-1,2} \quad | \quad \cdots \\ | \quad u_{1,N-1} \quad u_{2,N-1} \quad \cdots \quad u_{N-1,N-1}\Big], \tag{2.74}$$

is the reduced vector after the insertion of homogenous boundary conditions, and is of same ordering with Equation (2.69).

The block tridiagonal matrix T_1 has the form

$$T_1 = \begin{bmatrix} A_1 & B_1 & 0 & \cdots & 0 \\ B_1 & A_1 & B_1 & & \\ 0 & B_1 & A_1 & & \\ \vdots & & & & 0 \\ & & & & B_1 \\ 0 & \cdots & 0 & B_1 & A_1 \end{bmatrix}$$

where the matrices A_1 and B_1 tridiagonal matrices of size $(N-1) \times (N-1)$, and are given as:

$$A_1 = \begin{bmatrix} 20 & -4 & 0 & \cdots & 0 \\ -4 & 20 & -4 & & \\ 0 & -4 & 20 & & \\ \vdots & & & & 0 \\ & & & & -4 \\ 0 & \cdots & 0 & -4 & 20 \end{bmatrix}, \quad B_1 = \begin{bmatrix} -4 & -1 & 0 & \cdots & 0 \\ -1 & -4 & -1 & & \\ 0 & -1 & -4 & & \\ \vdots & & & & 0 \\ & & & & -1 \\ 0 & \cdots & 0 & -1 & -4 \end{bmatrix}.$$

On the other hand, T_2 has the form

$$T_2 = \begin{bmatrix} A_2 & I & 0 & \cdots & 0 \\ I & A_2 & I & & \\ 0 & I & A_2 & & \\ \vdots & & & & 0 \\ & & & & I \\ 0 & \cdots & 0 & I & A_2 \end{bmatrix}, \text{with} \quad A_2 = \begin{bmatrix} 8 & 1 & 0 & \cdots & 0 \\ 1 & 8 & 1 & & \\ 0 & 1 & 8 & & \\ \vdots & & & & 0 \\ & & & & 1 \\ 0 & \cdots & 0 & 1 & 8 \end{bmatrix},$$

where the identity matrix I and the matrix A_2 are of size $(N-1) \times (N-1)$.

When we use eigenvalue solvers for the sparse matrices in our MATLAB code, we get the results as presented in Table 2.2 which contains the smallest ten approximate eigenvalues $\lambda_{m,n}^h$ and exact eigenvalues $\lambda_{m,n}$ of Laplace EVP for $N = 128, 256, 512$ and 1024. The normalized errors $\varepsilon_{m,n}$ for each eigenvalue are also listed in the last column. It is seen from Table 2.2 that the approximate eigenvalues approach the exact eigenvalues $\lambda_{m,n}$ with an error less than 10^{-10} as the number of grid points N

increases. It can be observed from Table 2.1 and Table 2.2 that the approximate

Table 2.2: First ten ordered eigenvalues of Laplace EVP by the fourth order FDM.

m,n	$\lambda_{m,n}$	$N=128$	$N=256$	$N=512$	$N=1024$ ($\varepsilon_{m,n}$)
1,1	19.739208802	19.739208822	19.739208803	19.739208802	19.739208802(1.263e-11)
1,2	49.348022005	49.348021533	49.348021976	49.348022004	49.348022005(7.533e-12)
2,1	49.348022005	49.348021533	49.348021976	49.348022004	49.348022005(7.473e-12)
2,2	78.956835209	78.956836482	78.956835288	78.956835214	78.956835209(7.226e-13)
1,3	98.696044011	98.696035353	98.696043470	98.696043977	98.696044009(2.401e-11)
3,1	98.696044011	98.696035353	98.696043470	98.696043977	98.696044009(2.397e-11)
2,3	128.304857214	128.304857018	128.304857202	128.304857213	128.304857214(2.363e-12)
3,2	128.304857214	128.304857018	128.304857202	128.304857213	128.304857214(2.341e-12)
1,4	167.783274819	167.783220422	167.783271420	167.783274606	167.783274805(8.064e-11)
4,1	167.783274819	167.783220422	167.783271420	167.783274606	167.783274805(8.063e-11)

Table 2.3: Comparison of average computational times in seconds for the Laplace EVP with the relative error of $\lambda_{2,2}$.

Order of the method	$N=256$	$N=512$	$N=1024$
Second Order	0.42(5.0e-05)	1.85(1.3e-05)	8.52 (3.1e-06)
Fourth Order	0.71(1.0e-09)	3.43(6.2e-11)	16.69(7.2e-13)

eigenvalues obtained by fourth order finite difference scheme approach to the exact ones simpler than the ones obtained by the second order scheme. That is, more accurate results are obtained in the fourth order scheme when compared to the ones obtained by the second order scheme by using smaller number of grid points N. In Table 2.3, average of computational times in seconds for the simple eigenvalue $\lambda_{2,2}$ are given with the relative error, in parenthesis, obtained for the Laplace EVP. As can be seen from the table, the fourth order scheme is much more efficient than the second order one. In the fourth order method, it takes 0.71 seconds to obtain error 1.0e-09 for $N = 256$ while in the second order method it takes 8.52 seconds to reach the relative error at least 3.1e-06 for $N = 1024$. It can be concluded that the second order finite difference scheme is more time consuming since a finer mesh must be used to obtain the same accuracy in the fourth order scheme which requires less number of grid points.

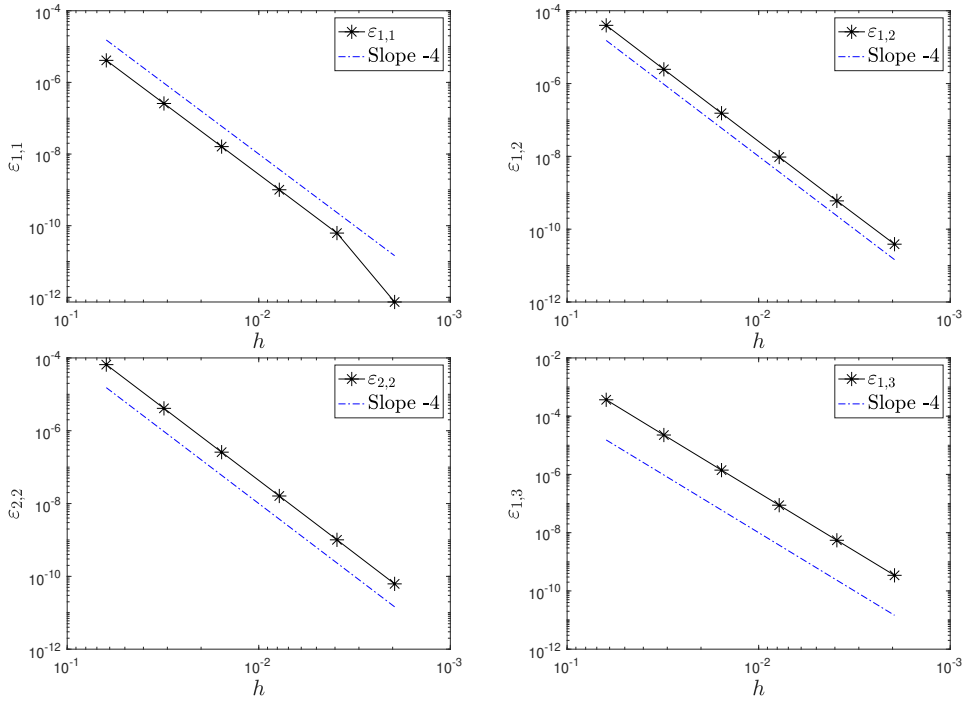

Figure 2.8: Convergence behavior of $\lambda_{m,n}^h$ to $\lambda_{m,n}$ versus the step size h in log-log scale by fourth order difference formula.

Figure 2.8 displays the convergence behavior of $\lambda_{m,n}^h$ to $\lambda_{m,n}$ in which the normalized error $\varepsilon_{m,n}$ are drawn in log-log scale. As expected due to use of a fourth order scheme, we end up with a fourth order convergence as the step size decreases. Furthermore, the approximate eigenfunctions $U^{m,n}$ corresponding to the eigenvalues $\lambda_{m,n}^h$ are analyzed and compared with the exact eigenfunctions $u^{m,n}$ in terms of contour plots. It is known that there exists only one eigenfunction to a simple eigenvalue $\lambda_{m,n} = (\pi m)^2 + (\pi n)^2$ when $m = n$. To see the good agreement of the approximate eigenfunctions $U^{1,1}$ and $U^{2,2}$ with the exact eigenfunctions $u^{1,1}$ and $u^{2,2}$, they are drawn in Figure 2.9 for the first two smallest simple eigenvalues $\lambda_{1,1}$ and $\lambda_{2,2}$.

On the other hand, it is observed from Table 2.2 that there are two different eigenvalues $\lambda_{m,n}^h$ that approximate the double eigenvalues $\lambda_{m,n} = \lambda_{n,m} = (\pi m)^2 + (\pi n)^2$ with $m \neq n$. It is known that the dimension of the exact eigenspace is two which is spanned by the exact eigenfunctions $u^{m,n}$ and $u^{n,m}$, $m \neq n$ corresponding to the double eigenvalues $\lambda_{m,n}$ and $\lambda_{n,m}$, $m \neq n$. However, the approximate eigenspace is made up of two different one-dimensional eigenspaces because the approximate eigenvalues are distinct [46]. As a result, in order to understand the convergence behavior of

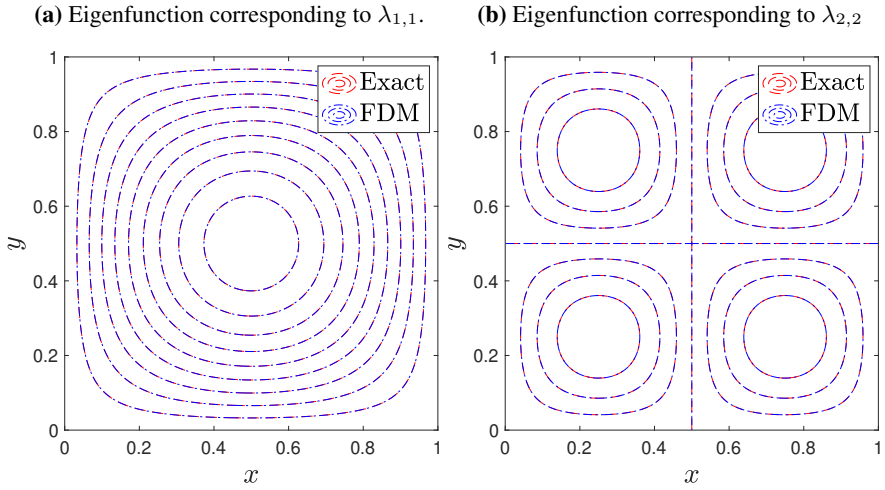

Figure 2.9: Comparison of the exact and approximate eigenfunctions corresponding to single eigenvalues $\lambda_{m,n}$, $m = n = 1, 2$

approximate eigenfunctions with double eigenvalues, it is necessary to establish that

$$\alpha^{(m,n)}u^{m,n} + \alpha^{(n,m)}u^{n,m} = \beta^{(m,n)}U^{m,n} + \beta^{(n,m)}U^{n,m}, \tag{2.75}$$

where $\alpha^{(m,n)}$, $\alpha^{(n,m)}$, $\beta^{(m,n)}$ and $\beta^{(n,m)}$ are constants for $m, n = 1, 2, \cdots$, and $m \neq n$, as explained in [47]. The matrix form of Equation 2.75 is

$$\begin{bmatrix} u^{m,n} & u^{n,m} \end{bmatrix} \begin{bmatrix} \alpha^{(m,n)} \\ \alpha^{(n,m)} \end{bmatrix} = \begin{bmatrix} U^{m,n} & U^{n,m} \end{bmatrix} \begin{bmatrix} \beta^{(m,n)} \\ \beta^{(n,m)} \end{bmatrix}. \tag{2.76}$$

When both sides in Equation 2.76 are multiplied with $\begin{bmatrix} (u^{m,n})^T & (u^{n,m})^T \end{bmatrix}^T$ from right, we obtain

$$\begin{bmatrix} (u^{m,n})^T u^{m,n} & (u^{m,n})^T u^{n,m} \\ (u^{n,m})^T u^{m,n} & (u^{n,m})^T u^{n,m} \end{bmatrix} \begin{bmatrix} \alpha^{(m,n)} \\ \alpha^{(n,m)} \end{bmatrix} = \begin{bmatrix} (u^{m,n})^T U^{m,n} & (u^{m,n})^T U^{n,m} \\ (u^{n,m})^T U^{m,n} & (u^{n,m})^T U^{n,m} \end{bmatrix} \begin{bmatrix} \beta^{(m,n)} \\ \beta^{(n,m)} \end{bmatrix}. \tag{2.77}$$

From the orthonormality of exact eigenfunctions, that is $(u^{m,n}) \cdot (u^{n,m}) = 1$ if $m = n$ and $(u^{m,n}) \cdot (u^{n,m}) = 0$ for $m \neq n$, Equation (2.77) becomes

$$\begin{bmatrix} \alpha^{(m,n)} \\ \alpha^{(n,m)} \end{bmatrix} = C \begin{bmatrix} \beta^{(m,n)} \\ \beta^{(n,m)} \end{bmatrix} \tag{2.78}$$

where the nonsingular matrix C can be evaluated using the known values $u^{m,n}$, $u^{n,m}$, $U^{m,n}$ and $U^{n,m}$,

$$C = \begin{bmatrix} (u^{m,n})^T U^{m,n} & (u^{m,n})^T U^{n,m} \\ (u^{n,m})^T U^{m,n} & (u^{n,m})^T U^{n,m} \end{bmatrix}. \tag{2.79}$$

If we assume that $\begin{bmatrix}\alpha^{(m,n)} & \alpha^{(n,m)}\end{bmatrix} = \begin{bmatrix}1 & 0\end{bmatrix}$, the constants $\begin{bmatrix}\beta^{(m,n)} & \beta^{(n,m)}\end{bmatrix}$ can be obtained from Equation (2.78), which reduces to

$$u^{m,n} = \beta^{(m,n)} U^{m,n} + \beta^{(n,m)} U^{n,m}. \tag{2.80}$$

Similarly, if we assume that $\begin{bmatrix}\alpha^{(m,n)} & \alpha^{(n,m)}\end{bmatrix} = \begin{bmatrix}0 & 1\end{bmatrix}$, one can obtain the constants $\begin{bmatrix}\beta^{(m,n)} & \beta^{(n,m)}\end{bmatrix}$ that give the second exact eigenfunction $u^{n,m}$ from Equation (2.78) as

$$u^{n,m} = \beta^{(m,n)} U^{m,n} + \beta^{(n,m)} U^{n,m}. \tag{2.81}$$

As it is figured out from Equations (2.80) and (2.81), the exact eigenfunctions are obtained as a linear combination of approximate eigenfunctions $U^{m,n}$ and $U^{n,m}$ through the constants $\beta^{(m,n)}$ and $\beta^{(n,m)}$. In order to confirm the obtained formulas (2.80) and (2.81) quantitatively, the approximate eigenfunctions $U^{m,n}$ and $U^{n,m}$, and the corresponding eigenfunctions are visualized in Figures 2.10, 2.11 and 2.12.

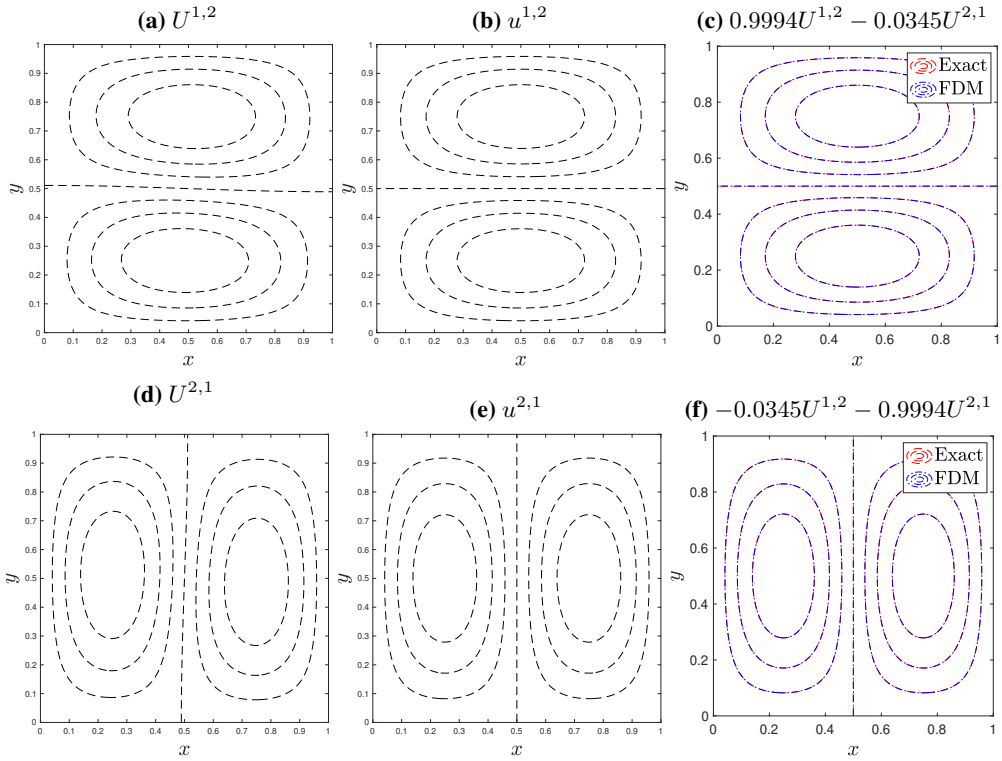

Figure 2.10: Eigenfunctions corresponding to the eigenvalues $\lambda_{1,2}$ and $\lambda_{2,1}$ of Laplace EVP.

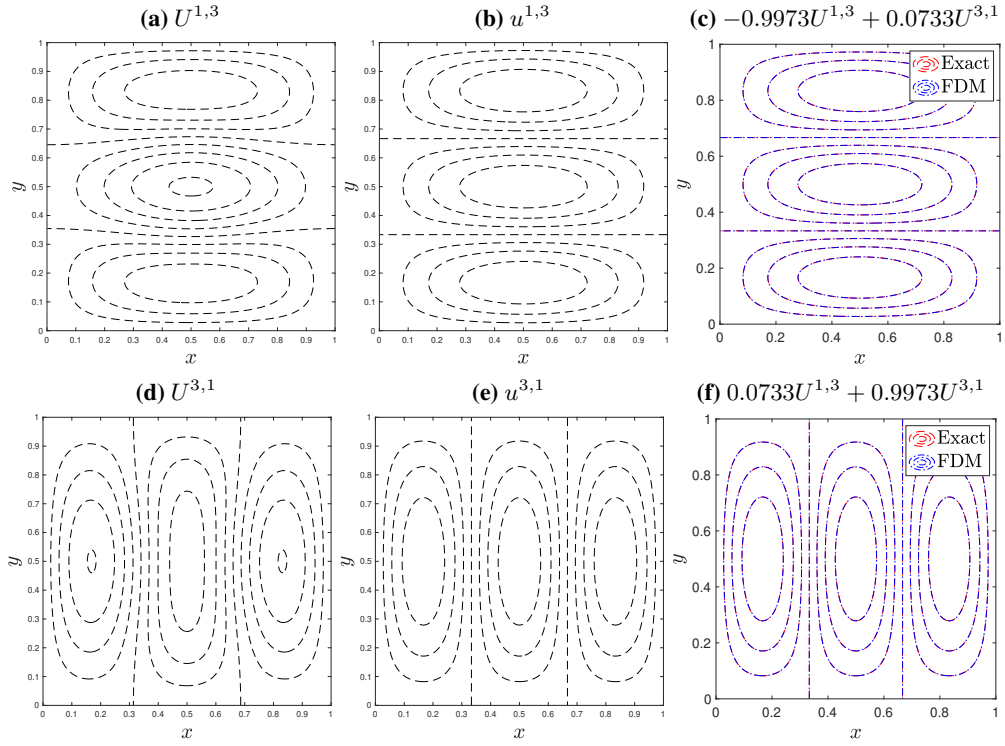

Figure 2.11: Eigenfunctions corresponding to the eigenvalues $\lambda_{1,3}$ and $\lambda_{3,1}$ of Laplace EVP.

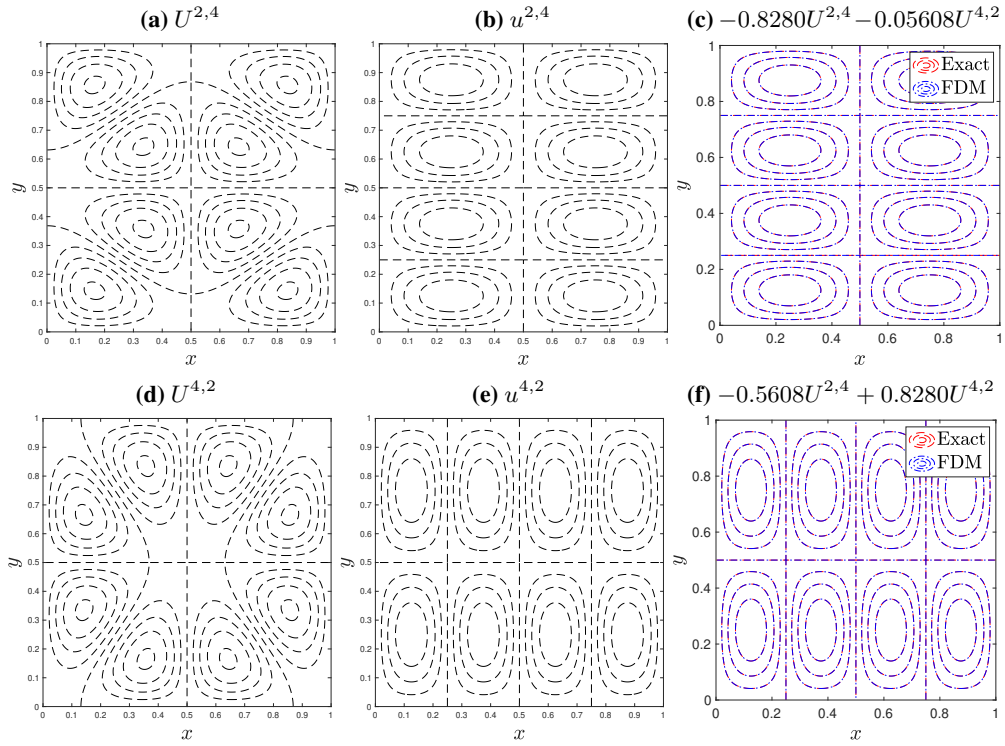

Figure 2.12: Eigenfunctions corresponding to the eigenvalues $\lambda_{2,4}$ and $\lambda_{4,2}$ of Laplace EVP.

The exact eigenfunctions obtained by Equations (2.80) and (2.81) in terms of linear combinations of the approximate eigenfunctions $U^{m,n}$ and $U^{n,m}$ for $m, n = 1, 2, 3$ are also illustrated at the right column of Figures 2.10, 2.11 and 2.12. It is observed that, some discrepancies occur between the exact eigenfunctions $u^{m,n}$, $u^{n,m}$ and the corresponding separate approximate eigenfunctions $U^{m,n}$ and $U^{n,m}$. However, the linear combinations of $U^{m,n}$ and $U^{n,m}$ provide reasonably well approximations for the corresponding exact eigenfunctions.

To conclude, in this chapter, the applications of the second and fourth order FDMs to the Poisson type equations including the Laplace eigenvalue problem in a square are given. The convergence behavior of the finite difference solutions to the exact ones are investigated in both Poisson Problem and Laplace EVP, and it is observed that the fourth order FDM yields better convergence rate compared to the second order FDM, as expected. Moreover, the finite difference solutions are in good agreement with the exact solutions, which validates the correctness of our computer codes as well as the effectiveness of the FDM for the solution of Poisson type equations, especially for the Laplace EVP.

CHAPTER 3

FINITE DIFFERENCE METHOD FOR THE STEKLOV EIGENVALUE PROBLEM

In this chapter, the Steklov EVP, one of the most important problems involving Laplace operator, will be examined on square domains with a variety of boundary conditions. The problem is a critical component of many applications and defined as: find the eigenvalues $\lambda \in \mathbb{R}$ and eigenfunctions $u \neq 0$ such that

$$\begin{cases} -\Delta u + \mu u = 0 & \text{in } \Omega, \\ \partial u/\partial n = \lambda \rho u & \text{on } \Gamma_\lambda, \\ \partial u/\partial n = 0 & \text{on } \Gamma_N, \end{cases} \tag{3.1}$$

where n denotes the unitary outward normal to the domain Ω which is in $\mathbb{R}^d$, $d = 1, 2, 3$ with the boundary $\partial\Omega = \Gamma_\lambda \cup \Gamma_N$ where Γ_λ and Γ_N are disjoint open subsets of $\partial\Omega$ with $\Gamma_\lambda \neq \emptyset$, and μ and ρ are given spatially dependent variables. For instance, in the case of a vibrating free membrane, ρ is a weight function indicating the density of the mass concentrated along the boundary.

It can be seen from Equation (2.44) and Equation (3.1) that the Steklov EVP differs from the Laplace EVP in the place of the eigenvalues. The eigenvalues occur on the boundary conditions in Steklov EVP whereas they are on the differential equation in the Laplace EVP.

The presentation of the FDM approximation of the Steklov EVP is the focus of the present chapter. Primarily, the most known form of the Steklov EVP with mixed type boundary condition involving the spectral parameter λ given on the whole boundary, that is $\partial\Omega = \Gamma_\lambda$ is considered in Section 3.1 on square domains. The discretization of the differential equation is performed by using both second and fourth order

central differences for the Laplace operator in Section 3.1.a and 3.1.b, respectively. The mixed type boundary condition involving the first order partial derivatives is approximated by either backward-forward difference formulas of first order or by using second and fourth order central difference formulas. In Section 3.2, the mixed type Steklov EVP defined on a square domain is solved also by using the fourth order difference formulas for the differential equation while a combination of either first and second or second and fourth order formulas are employed for the discretization of the derivative boundary conditions. In the mixed problem the boundary of the domain is divided into two disjoint parts, namely $\partial\Omega = \Gamma_\lambda \cup \Gamma_N$ having different boundary conditions. That is, the mixed type boundary condition involving spectral parameter λ is taken on Γ_λ, and on Γ_N the Neumann type boundary condition is taken into account. The obtained finite difference solutions are presented in terms of convergence rate of eigenvalues and contour plots of eigenfunctions in the given computational domain.

Throughout this chapter to indicate the order of finite difference formulas applied to the differential operator and the boundary conditions, we use the abbreviation O_iB_j or $O_iB_{j,k}$. Here, suffix i shows the order of difference formulas employed for the discretization of differential operator (O), while the suffices j, k show the order of difference formulas used in approximating the derivative boundary conditions. For example, $O_2B_{1,2}$ implies that a second order difference formula is used for the discretization of the differential equation, while in the approximation of the derivative boundary conditions a combination of first and second order difference formulas are applied.

3.1 The Standard Steklov Eigenvalue Problem

In this section, the most popular form of the Steklov EVP involving only non-homogenous type boundary condition with the eigenvalue parameter λ given as

$$\begin{cases} -\Delta u + \mu u = 0 & \text{in } \Omega, \\ \dfrac{\partial u}{\partial n} = \lambda \rho u & \text{on } \partial\Omega = \Gamma_\lambda, \end{cases} \tag{3.2}$$

is considered on square domains for various values of ρ and μ.

First, the code validation is performed for the pure (simplified) Steklov EVP, when

$\mu = 0$ and $\rho = 1$, defined on the square $\Omega = [-1, 1] \times [-1, 1]$, where the problem has the exact solution. That is, we solve the simplified Steklov EVP

$$\begin{cases} \Delta u = 0 & \text{in } \Omega, \\ \dfrac{\partial u}{\partial n} = \lambda u & \text{on } \partial\Omega \end{cases} \tag{3.3}$$

by using fourth order central difference formulas (2.21)-(2.23) to approximate the differential equation, while the mixed type boundary condition with dependence on the eigenvalue λ is approximated by the second order central difference formulas (2.14)-(2.15), that is we use the method O_4B_2.

The exact solution of the problem (3.3) can be found in the work of Girouard [11] and is tabulated here in Table 3.1. Once the equations in the mid column of Table 3.1 are solved for α, the corresponding eigenfunctions and eigenvalues can be obtained.

Table 3.1: Conditions for exact eigenvalues and eigenspace of standard Steklov EVP on $\Omega = [-1, 1] \times [-1, 1]$ when $\rho = 1$ and $\mu = 0$.

Eigenspace basis	Conditions on α	Eigenvalues
$\cos(\alpha x)\cosh(\alpha y)$ $\cos(\alpha y)\cosh(\alpha x)$	$\tan(\alpha) = -\tanh(\alpha)$	$\alpha\tanh(\alpha)$
$\sin(\alpha x)\cosh(\alpha y)$ $\sin(\alpha y)\cosh(\alpha x)$	$\tan(\alpha) = \coth(\alpha)$	$\alpha\tanh(\alpha)$
$\cos(\alpha x)\sinh(\alpha y)$ $\cos(\alpha y)\sinh(\alpha x)$	$\tan(\alpha) = -\coth(\alpha)$	$\alpha\coth(\alpha)$
$\sin(\alpha x)\sinh(\alpha y)$ $\sin(\alpha y)\sinh(\alpha x)$	$\tan(\alpha) = \tanh(\alpha)$	$\alpha\coth(\alpha)$
xy		1

Table 3.2: The smallest six eigenvalues of standard Steklov EVP with the corresponding values of α.

i	α_i	λ_i	$N = 128$	$N = 256$	$N = 512$	$N = 1024$
1	0	0	-6.730e-14	-3.717e-13	-1.346e-12	-5.924e-12
2	-0.937552	0.688252	0.688217 +-0.000031i	0.688249 +0.000000i	0.688266 +0.000000i	0.688251+ 0.000000i
3	-0.937552	0.688252	0.688217 +0.000031i	0.688254 +0.000000i	0.688266 +0.000000i	0.688257+ 0.000000i
4	-	1	1.000106 +0.000000i	1.000002 +0.000000i	1.000000 +0.000000i	0.999998+ 0.000000i
5	-2.365002	2.323638	2.317733 +0.000000i	2.323544 +0.000000i	2.323867 +0.000000i	2.323645+ 0.000000i
6	-2.365002	2.323638	2.323876 +0.000000i	2.323722 +0.000000i	2.323867 +0.000000i	2.323728+ 0.000000i

The smallest six eigenvalues and corresponding α values are given in Table 3.2. It is observed that the approximate eigenvalues are obtained as complex numbers with

almost zero imaginary parts especially at high values of subintervals N. The reason for obtaining imaginary parts is having a coefficient matrix which is not symmetric in the resulting finite difference system of equations due to mixed type boundary conditions.

The well agreement of the finite difference approximation with the exact solution is displayed in Figure 3.1, Figure 3.2 and Figure 3.3 in terms of contour plots of eigenfunctions for $N = 1024$. In Figure 3.1, the exact eigenfunction u_4 corresponding to simple eigenvalue $\lambda_4 = 1$ is drawn with the approximate eigenfunction U_4.

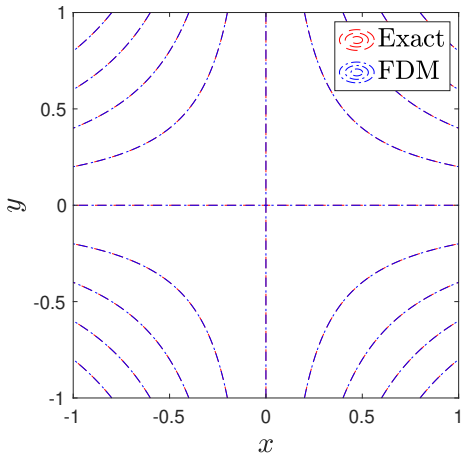

Figure 3.1: Comparison of the exact and the FD eigenfunctions corresponding to simple eigenvalue $\lambda_4 = 1$ for Steklov EVP with $\rho = 1$, $\mu = 0$.

On the other hand, the eigenfunctions corresponding to the double eigenvalues $\lambda_2 = \lambda_3 = 0.688252$ and $\lambda_5 = \lambda_6 = 2.323638$ are drawn in Figure 3.2 and Figure 3.3, respectively. It is observed, in Figures 3.2 and 3.3, that the contour plots of the approximate eigenfunctions (U_2,U_3) and (U_5,U_6), corresponding to double eigenvalues $\lambda_2 = \lambda_3$ and $\lambda_5 = \lambda_6$, do not match with the exact eigenfunctions (u_2,u_3) and (u_5,u_6), respectively, due to the fact explained in Chapter 2, Section 2.2.b.2 for the double eigenvalues of Laplace EVP. That is, there are two linearly independent eigenfunctions for the double eigenvalues, so that, any linear combinations of them also produce an eigenfunction which may agree with the exact eigenfunction. The appropriate coefficients of the linear combination are found by the technique explained in Section 2.2.b.2, and the obtained results are drawn on the third columns of Figures 3.2 and 3.3. Thus, it is seen that the finite difference method gives reasonably well approximations to the exact solutions of the standard Steklov eigenvalue problem with $\rho = 1$ and $\mu = 0$ in the square domain $\Omega = [-1, 1] \times [-1, 1]$.

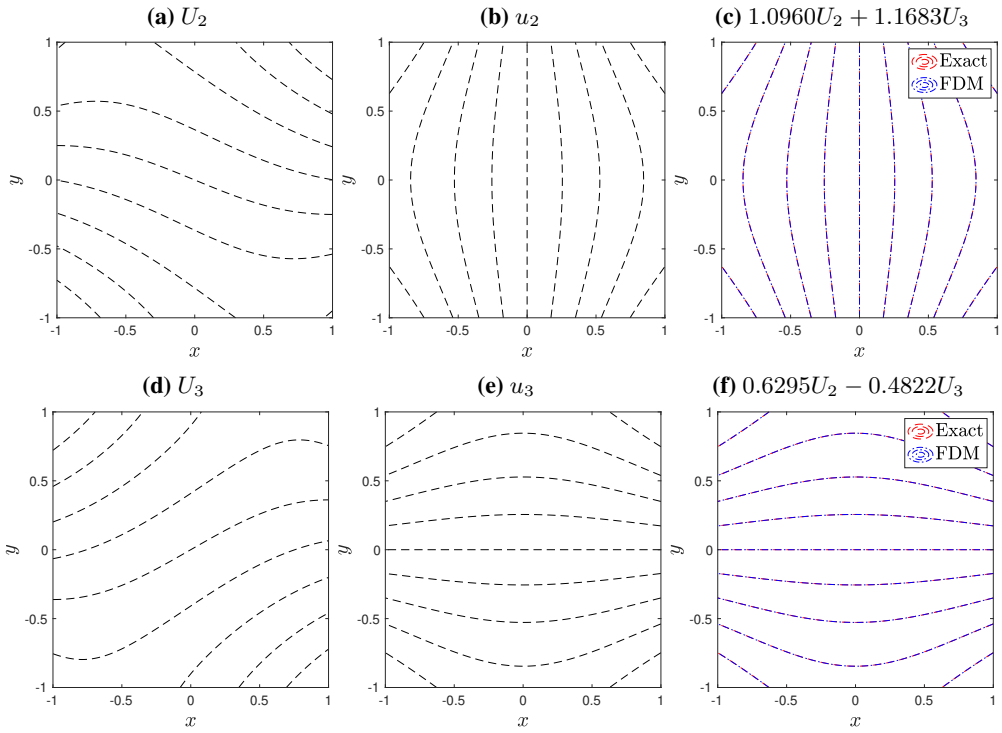

Figure 3.2: Eigenfunctions corresponding to double eigenvalues $\lambda_2 = \lambda_3$ of Steklov EVP with $\rho = 1$, $\mu = 0$.

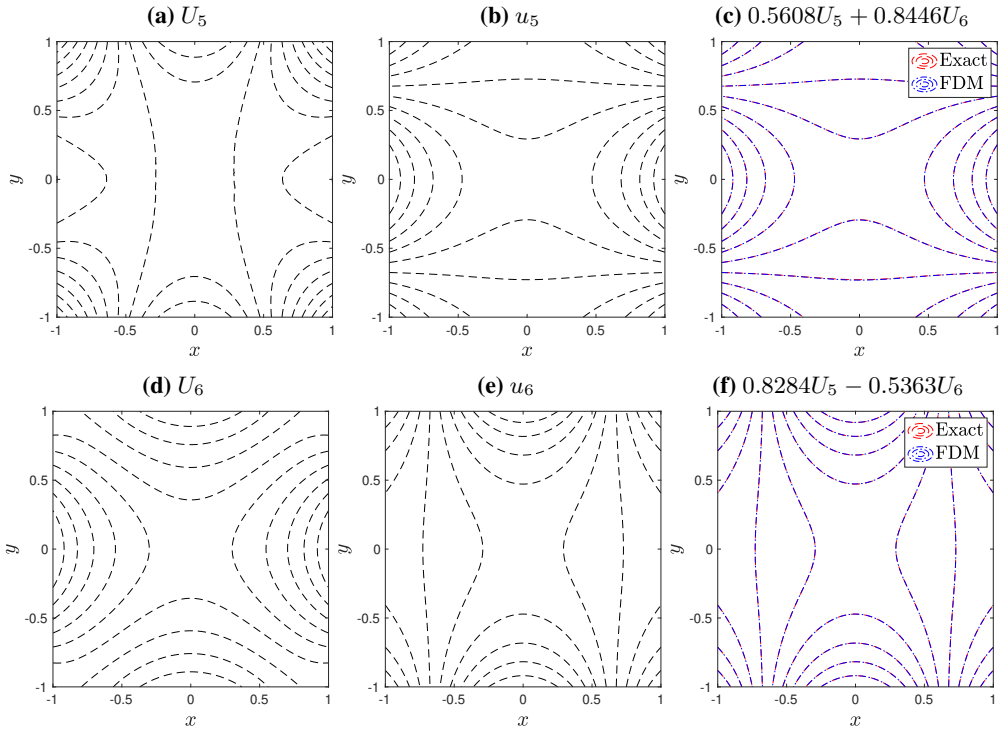

Figure 3.3: Eigenfunctions corresponding to double eigenvalues $\lambda_5 = \lambda_6$ of Steklov EVP with $\rho = 1$, $\mu = 0$.

In the rest of the section, the second and fourth order finite difference approximations to the standard Steklov EVP (3.2) with non-zero μ values are considered on the square domain $\Omega = [0, \sqrt{2}] \times [0, \sqrt{2}]$ to observe the convergence behavior under different finite difference formulas for the approximation of the boundary conditions.

3.1.a Approximation of Steklov EVP by Second Order Central Difference Formulas

In this section, the second order central difference formulas (2.18)-(2.19) are utilized to approximate the Poisson type differential equation given in Equation (3.2) with right hand side function $f(x, y, u) = -\mu u$ as explained in Chapter 2; Section 2.2.a.1 for the Poisson equation. When the computational domain $\Omega = [0, \sqrt{2}] \times [0, \sqrt{2}]$ is discretized by using a uniform mesh of N subintervals of equal length $h = k = l/N$ ($l = \sqrt{2}$) in both x and y-directions, and the application of the central difference formulas to second order partials results in the following finite difference equation:

$$\frac{U_{i+1,j} - 2U_{i,j} + U_{i-1,j}}{h^2} + \frac{U_{i,j+1} - 2U_{i,j} + U_{i,j-1}}{h^2} - \mu U_{i,j} = 0, \tag{3.4}$$

which can be written as

$$(-4 - h^2\mu)U_{i,j} + U_{i+1,j} + U_{i-1,j} + U_{i,j+1} + U_{i,j-1} = 0, \tag{3.5}$$

at an interior point $(x_i, y_j) \in \Omega$.

On the other hand, the mixed type boundary condition with eigenvalue parameter λ can be handled by using different finite difference formulas for the approximation of first order partial derivative $\partial u/\partial n$ along the boundary of computational domain Ω. Thus, the application of forward and backward difference formulas are explained in Section 3.1.a.1, while the use of central difference formulas are given in Section 3.1.a.2.

3.1.a.1 Approximation of the Boundary Condition by First Order Backward-Forward Difference Formulas (O_2B_1)

The derivative boundary condition is approximated by either forward differences (2.7)-(2.8) or backward differences (2.11)-(2.12) along suitable boundaries in order

to avoid the occurrence of ghost points in the resulting system of finite difference equations.

The boundary conditions at $x = 0$ and $y = 0$ are

$$\frac{\partial u}{\partial n} = -\frac{\partial u}{\partial x} = \lambda \rho u \quad \text{and} \quad \frac{\partial u}{\partial n} = -\frac{\partial u}{\partial y} = \lambda \rho u. \tag{3.6}$$

Applying the forward difference formulas (2.7)-(2.8) to the partial derivatives $\partial u/\partial x$ at $x = 0$ and to $\partial u/\partial y$ at $y = 0$ gives

$$U_{0,j} = \frac{1}{1 - h\rho\lambda} U_{1,j} \quad \text{and} \quad U_{i,0} = \frac{1}{1 - h\rho\lambda} U_{i,1}. \tag{3.7}$$

On the other hand, the boundary conditions at $x = \sqrt{2}$ and $y = \sqrt{2}$ are

$$\frac{\partial u}{\partial n} = \frac{\partial u}{\partial x} = \lambda \rho u \quad \text{and} \quad \frac{\partial u}{\partial n} = \frac{\partial u}{\partial y} = \lambda \rho u. \tag{3.8}$$

Application of the backward difference formulas (2.11)-(2.12) to the partial derivatives $\partial u/\partial x$ at $x = \sqrt{2}$ and to $\partial u/\partial y$ at $y = \sqrt{2}$, respectively, results in

$$U_{N,j} = \frac{1}{1 - h\rho\lambda} U_{N-1,j} \quad \text{and} \quad U_{i,N} = \frac{1}{1 - h\rho\lambda} U_{i,N-1}. \tag{3.9}$$

Once the difference equation (3.5) is written for $i, j = 1, \cdots, N-1$ and the discretized boundary conditions (3.7) and (3.9) are inserted, we obtain the system of linear equations which can be expressed in the matrix form as

$$AU = \tilde{\lambda} BU. \tag{3.10}$$

This is the generalized eigenvalue problem with $\tilde{\lambda} = h\rho\lambda$ and the coefficient matrix $A = T + B$ is of size $(N+1)^2 \times (N+1)^2$. Here, U is the reduced vector after the insertion of boundary conditions and involves the discrete eigenvector at the interior nodes in the following order:

$$U^T = \Big[U_{1,1} \quad u_{2,1} \quad \cdots \quad U_{N-1,1} \quad | \quad U_{1,2} \quad U_{2,2} \quad \cdots \quad U_{N-1,2} \quad | \quad \cdots \\ | \quad U_{1,N-1} \quad U_{2,N-1} \quad \cdots \quad U_{N-1,N-1} \Big]. \tag{3.11}$$

The matrix T is the block tridiagonal matrix given as

$$T = \begin{bmatrix} C & I & 0 & \cdots & 0 \\ I & C & I & \ddots & \vdots \\ 0 & I & C & \ddots & 0 \\ \vdots & \ddots & \ddots & \ddots & I \\ 0 & \cdots & 0 & I & C \end{bmatrix}, \text{ where } \quad C = \begin{bmatrix} k & 1 & 0 & \cdots & 0 \\ 1 & k & 1 & \ddots & \vdots \\ 0 & 1 & k & \ddots & 0 \\ \vdots & \ddots & \ddots & \ddots & 1 \\ 0 & \cdots & 0 & 1 & k \end{bmatrix},$$

with $k = -4 - h^2\mu$, and I is the identity matrix of size $(N-1) \times (N-1)$.

On the other hand, the matrix B has the block diagonal form

$$B = \begin{bmatrix} D & 0 & 0 & \cdots & 0 \\ 0 & E & 0 & \ddots & \vdots \\ 0 & 0 & \ddots & \ddots & 0 \\ \vdots & \ddots & \ddots & E & 0 \\ 0 & \cdots & 0 & 0 & D \end{bmatrix}$$

where the matrices D and E diagonal matrices of size $(N-1)\times(N-1)$, and obtained as $D = \text{diag}(2, 1, 1, \cdots, 1, 2)$ and $E = \text{diag}(1, 0, 0, \cdots, 0, 1)$.

Table 3.3: First ten ordered eigenvalues of Steklov EVP by O_2B_1 for $\mu = -4$ and $\rho = -1$.

i	Ref.(λ_i)	$N = 500$	$N = 1000$	$N = 1500$	$N = 2000$	$N = 2500$	$N = 3000$	$N = 3500$
1	-0.2127	-0.2162	-0.2142	-0.2136	-0.2132	-0.2130	-0.2129	-0.2128
2	-0.2127	-0.2162	-0.2142	-0.2136	-0.2132	-0.2130	-0.2129	-0.2128
3	-0.9085	-0.9121	-0.9101	-0.9094	-0.9091	-0.9089	-0.9087	-0.9086
4	2.2013	2.1928	2.1977	2.1993	2.2001	2.2006	2.2009	2..2011
5	-2.7699	-2.7767	-2.7728	-2.7715	-2.7709	-2.7705	-2.7702	-2.7700
6	-2.7699	-2.7767	-2.7728	-2.7715	-2.7709	-2.7705	-2.7702	-2.7700
7	-2.9195	-2.9263	-2.9224	-2.9211	-2.9205	-2.9201	-2.9198	-2.9197
8	-2.9195	-2.9263	-2.9224	-2.9211	-2.9205	-2.9201	-2.9198	-2.9197
9	-5.2285	-5.2389	-5.2330	-5.2310	-5.2300	-5.2295	-5.2291	-5.2288
10	-5.2285	-5.2389	-5.2330	-5.2310	-5.2300	-5.2295	-5.2291	-5.2288

When the generalized eigenvalue problem solver for the sparse matrices in MATLAB is used, we get the approximate values of eigenvalues as presented in Table 3.3 and Table 3.4. These tables contain the smallest ten approximate eigenvalues λ_i^h and the reference values λ_i of the standard Steklov EVP, which has no exact solution, on

$\Omega = [0, \sqrt{2}] \times [0, \sqrt{2}]$ for $\mu = -4$ and $\mu = -4 - 4i$ with $\rho = -1$. Thus, to investigate the convergence behavior of approximate solution λ_i^h, the reference values λ_i are

Table 3.4: First ten ordered eigenvalues of Steklov EVP by O_2B_1 for $\mu = -4 - 4i$ and $\rho = -1$.

i	Ref.(λ_i)	$N = 500$	$N = 1000$	$N = 1500$
1	-0.343983+0.849909i	-0.346790+0.847399i	-0.344919+0.849072i	-0.344295+0.849630i
2	-0.343983+0.849909i	-0.346790+0.847399i	-0.344919+0.849072i	-0.344295+0.849630i
3	-0.950817+0.539390i	-0.952935+0.537271i	-0.951524+0.538683i	-0.951053+0.539154i
4	0.685845+2.494587i	0.683723+2.492460i	0.685137+2.493878i	0.685609+2.494351i
5	-2.795741+0.539341i	-2.793367+0.535186i	-2.794953+0.537954i	-2.795478+0.538878i
6	-2.795741+0.539341i	-2.793367+0.535186i	-2.794953+0.537954i	-2.795478+0.538878i
7	-2.930115+0.472929i	-2.926960+0.469209i	-2.929067+0.471687i	-2.929766+0.472515i
8	-2.930115+0.472929i	-2.926960+0.469209i	-2.929067+0.471687i	-2.929766+0.472515i
9	-5.228102+0.328378i	-5.207919+0.324207i	-5.221378+0.326983i	-5.225861+0.327912i
10	-5.228102+0.328378i	-5.207919+0.324207i	-5.221378+0.326983i	-5.225861+0.327912i

taken as the approximate solutions obtained by using the largest value of N that our code can handle. That is, the reference values λ_i are obtained by taking $N = 4096$ for the selfadjoint case where μ is a real number (specifically $\mu = -4$), and $N = 2048$ for the non-selfadjoint case where μ is a complex number (specifically $\mu = -4 - 4i$) in numerical simulations. For the selfadjoint case, the approximate solutions λ_i^h are obtained using the number of grid points $N = 500, 100, \cdots, 3500$ whereas in the non-selfadjoint case $N = 500, 1000$ and 1500 are used. It can be observed from Table 3.3 that as the number of grid points N increases, the approximate eigenvalues λ_i^h also increase, and they approach to the reference values λ_i. Also, a similar behavior can be seen for the non-selfadjoint case from Table 3.4, in which both the real and imaginary parts approach to the reference values as N increases. The normalized relative errors $\varepsilon_i = \left| \dfrac{\lambda_i - \lambda_i^h}{\lambda_i} \right|$, where λ_i denotes the reference value obtained by using $N = 4096$ subintervals when $\mu = -4$ and by using $N = 2000$ subintervals when $\mu = -4 - 4i$, and ${\lambda_i}^h$ is the approximate solution for the i-th eigenvalue, are shown in Figures 3.4 and 3.5 for $\mu = -4$ and $\mu = -4 - 4i$, respectively. From Table 3.3, it can be seen that there are double eigenvalues (λ_1,λ_2), (λ_5,λ_6), (λ_7,λ_8) and (λ_9,λ_{10}), so the error figures are given only once for each couple, namely $\lambda_1, \lambda_5, \lambda_7$ and λ_9. These figures display that the convergence behavior of the approximate eigenvalue λ_i is of order

$O(h)$ since they show a linear behavior parallel to a line with slope $m = -1$ in each figure.

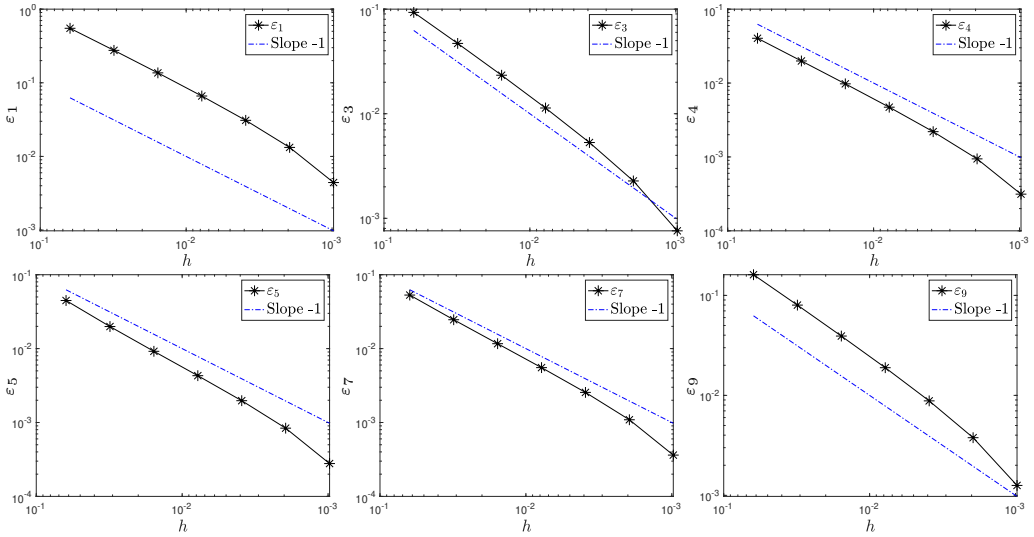

Figure 3.4: Convergence behavior of λ_i^h to λ_i versus the step size h in log-log scale for $\mu = -4$ and $\rho = -1$ by O_2B_1.

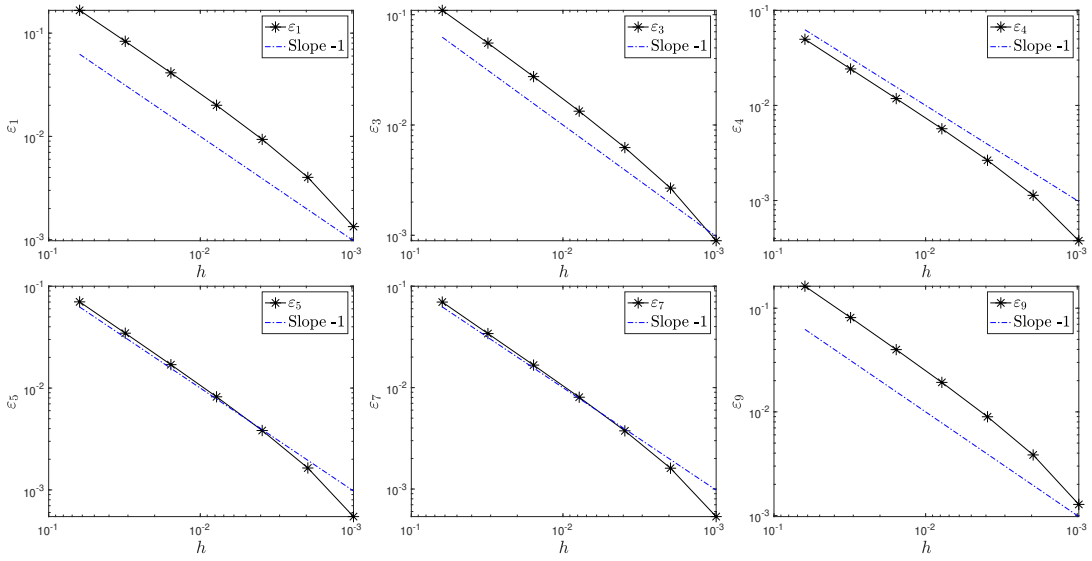

Figure 3.5: Convergence behavior of λ_i^h to λ_i versus the step size h in log-log scale for $\mu = -4 - 4i$ and $\rho = -1$ by O_2B_1.

To summarize, from the results given in this section, it is observed that as the number N increases, the eigenvalues approach to the values obtained for the largest N values with the order $O(h)$ in both selfadjoint and non-selfadjoint cases.

3.1.a.2 Approximation of the Boundary Condition by Second Order Central Difference Formula (O_2B_2)

In this section, the second order central difference formulas (2.14)-(2.15) are employed for the approximation of first order derivatives in the mixed type boundary conditions. The boundary conditions along the boundaries at $x = 0, \sqrt{2}$ given in Equations (3.6) and (3.8) are discretized by using the central difference formula (2.14), and we obtain

$$U_{-1,j} = 2h\rho\lambda U_{0,j} + U_{1,j}, \tag{3.12}$$

$$U_{N+1,j} = 2h\rho\lambda U_{N,j} + U_{N-1,j}. \tag{3.13}$$

Similarly, the application of central difference formula (2.15) to the y-derivatives in Equations (3.6) and (3.8) along the boundaries $y = 0$ and $y = \sqrt{2}$ result in

$$U_{i,-1} = 2h\rho\lambda U_{i,0} + U_{i,1}, \tag{3.14}$$

$$U_{i,N+1} = 2h\rho\lambda U_{i,N} + U_{i,N-1}. \tag{3.15}$$

Thus, the ghost points $U_{-1,j}$, $U_{N+1,j}$, $U_{i,-1}$, $U_{i,N+1}$ arising by writing the difference equation (3.5) for $i, j = 0, 1, 2, \cdots, N$ are removed by using the discretized boundary equations (3.12)-(3.15). Thus, we end up with a linear system of $(N+1) \times (N+1)$ equations which can be written in the matrix form as

$$AU = \tilde{\lambda} BU, \tag{3.16}$$

which is again a generalized eigenvalue problem with $\tilde{\lambda} = h\rho\lambda$. The vector

$$U^T = \Big[U_{0,0} \quad U_{1,0} \quad \cdots \quad U_{N,0} \quad | \quad U_{0,1} \quad U_{1,1} \quad \cdots \quad U_{N,1} \quad | \quad \cdots \quad | \quad U_{0,N} \quad U_{1,N} \quad \cdots \quad U_{N,N}\Big] \tag{3.17}$$

is the reduced unknown vector obtained after the insertion of the boundary conditions. The coefficient matrix A has the form

$$A = \begin{bmatrix} C & 2I & 0 & \cdots & \cdots & 0 \\ I & C & I & \ddots & & \vdots \\ 0 & I & C & I & \ddots & \vdots \\ \vdots & \ddots & I & C & I & 0 \\ \vdots & & \ddots & I & C & I \\ 0 & \cdots & \cdots & 0 & 2I & C \end{bmatrix}, \text{ where } \quad C = \begin{bmatrix} k & 2 & 0 & \cdots & \cdots & 0 \\ 1 & k & 1 & \ddots & & \vdots \\ 0 & 1 & k & 1 & \ddots & \vdots \\ \vdots & \ddots & 1 & k & 1 & 0 \\ \vdots & & \ddots & 1 & k & 1 \\ 0 & \cdots & \cdots & 0 & 2 & k \end{bmatrix}$$

with $k = -4 - h^2\mu$ and I is the identity matrix of size $(N+1) \times (N+1)$. On the other hand, the matrix B has the form

$$B = \begin{bmatrix} D & 0 & 0 & \cdots & \cdots & 0 \\ 0 & E & 0 & \ddots & & \vdots \\ 0 & 0 & \ddots & \ddots & \ddots & \vdots \\ \vdots & \ddots & \ddots & \ddots & 0 & \vdots \\ \vdots & & \ddots & E & 0 & \vdots \\ 0 & \cdots & 0 & 0 & D & \end{bmatrix},$$

where D and E are diagonal matrices of sizes $(N+1) \times (N+1)$, that is $D = \text{diag}(-4, -2, -2, \cdots, -2, -4)$ and $E = \text{diag}(-2, 0, 0, \cdots, 0, -2)$.

When the generalized eigenvalue problem solver for sparse matrices in MATLAB are used, we obtain the approximate eigenvalues of the standard Steklov EVP shown in Table 3.5 and Table 3.6. These tables contain the smallest ten approximate eigenvalues λ_i^h for $N = 512, 1024, 2048$ with $\mu = -4$ and $\mu = -4 - 4i$, respectively. Also, the reference values λ_i in the second column's of tables are taken as the approximate solutions using $N = 4096$ number of subintervals for $\mu = -4$ and $N = 2048$ for $\mu = -4 - 4i$. It is observed that the results obtained by using central difference for the boundary conditions are more accurate than the ones obtained in the previous section in which forward-backward differences are employed for the boundary conditions.

Table 3.5: Eigenvalues of Steklov EVP by O_2B_2 for $\mu = -4$ and $\rho = -1$.

i	Ref.(λ_i)	$N = 512$	$N = 1024$	$N = 2048$
1	-0.21225212	-0.21224883	-0.21225133	-0.21225196
2	-0.21225212	-0.21224883	-0.21225133	-0.21225196
3	-0.90805604	-0.90805308	-0.90805534	-0.90805590
4	2.20250711	2.20250601	2.20250685	2.20250706
5	-2.76894676	-2.76893602	-2.76894420	-2.76894625
6	-2.76894676	-2.76893602	-2.76894420	-2.76894625
7	-2.91855097	-2.91854695	-2.91855001	-2.91855078
8	-2.91855097	-2.91854695	-2.91855001	-2.91855078
9	-5.22710045	-5.22713509	-5.22710870	-5.22710210
10	-5.22710045	-5.22713509	-5.22710870	-5.22710210

Table 3.6: Eigenvalues of Steklov EVP by O_2B_2 for $\mu = -4 - 4i$ and $\rho = -1$.

i	Ref.(λ_i)	$N = 500$	$N = 1000$	$N = 1500$
1	-0.343046 +0.850747i	-0.343042 +0.850748i	-0.343045 +0.850747i	-0.343046+ 0.850747i
2	-0.343046 +0.850747i	-0.343042 +0.850748i	-0.343045 +0.850747i	-0.343046+ 0.850747i
3	-0.901545 -1.391922i	-0.901545 -1.391921i	-0.901545 -1.391922i	-0.901545 -1.391922i
4	0.686552 +2.495294i	0.686551 +2.495288i	0.686552 +2.495293i	0.686552+ 2.495293i
5	-2.796523 +0.540731i	-2.796511 +0.540746i	-2.796521 +0.540734i	-2.796523+ 0.540732i
6	-2.796523 +0.540731i	-2.796511 +0.540746i	-2.796521 +0.540734i	-2.796523+ 0.540732i
7	-2.931161 +0.474174i	-2.931155 +0.474187i	-2.931159 +0.474176i	-2.931160+ 0.474174i
8	-2.931161 +0.474174i	-2.931155 +0.474187i	-2.931159 +0.474176i	-2.931160+ 0.474174i
9	-5.234826 +0.329778i	-5.234859 +0.329808i	-5.234832 +0.329784i	-5.234827+ 0.329779i
10	-5.234826 +0.329778i	-5.234859 +0.329808i	-5.234832 +0.329784i	-5.234827+ 0.329779i

Figure 3.6 and Figure 3.7 illustrate the normalized errors ε_i of λ_i found by second order central difference formula in log-log scale, respectively for $\mu = -4$ and $\mu = -4-4i$. These figures indicate that the approximate eigenvalue λ_i^h has a convergence behavior of order $O(h^2)$ for both real and complex values of μ.

As a conclusion, the use of central difference approximations for the discretization of the boundary conditions advances the convergence behavior of the approximate eigenvalues λ_i^h to the reference values λ_i, to of order $O(h^2)$ for both complex and

real values of μ when compared to the order $O(h)$ obtained by using forward and backward difference approximations to the boundary conditions.

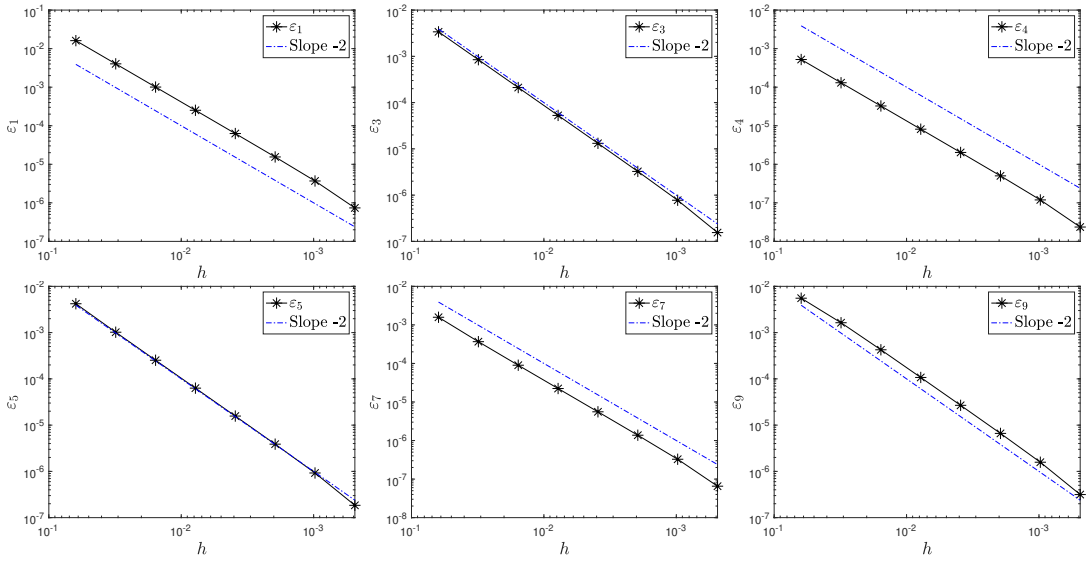

Figure 3.6: Convergence behavior of λ_i^h to λ_i versus the step size h in log-log scale for $\mu = -4$ and $\rho = -1$ by O_2B_2.

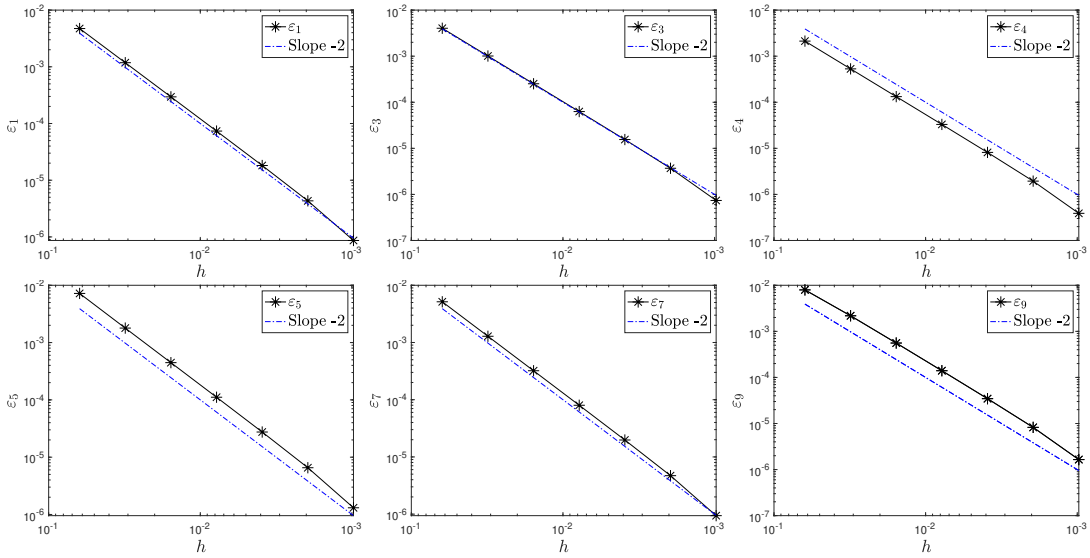

Figure 3.7: Convergence behavior of λ_i^h to λ_i versus the step size h in log-log scale for $\mu = -4 - 4i$ and $\rho = -1$ by O_2B_2.

3.1.b Approximation of Steklov EVP by Fourth Order Central Difference Formulas $(O_4B_{2,4})$

In the discretization of the differential equation in (3.2), the fourth order central difference formulas (2.21)-(2.23) are applied at point (x_i, y_j) by taking N equal length

subintervals in x and y-directions, that is we take $h = k = \sqrt{2}/N$, as in Section 3.1.a. As a result, the following finite difference equation

$$\frac{1}{12h^2}(-U_{i+2,j} + 16U_{i+1,j} - 30U_{i,j} + 16U_{i-1,j} - U_{i-2,j}) + \frac{1}{12h^2}(-U_{i,j+2} + 16U_{i,j+1} \\ -30U_{i,j} + 16U_{i,j-1} - U_{i,j-2}) - \mu U_{i,j} = 0 \tag{3.18}$$

is obtained at the mesh points (x_i, y_j), $i, j = 1, 2, \cdots, N$. The difference equation can also be written as

$$(-60 - 12h^2\mu)U_{i,j} - U_{i+2,j} + 16U_{i+1,j} + 16U_{i-1,j} - U_{i-2,j} - U_{i,j+2} \\ +16U_{i,j+2} + 16U_{i,j-1} - U_{i,j-2} = 0. \tag{3.19}$$

On the other hand, the boundary conditions are approximated by using with both the second order central difference formulas (2.14)-(2.15) and the fourth order formulas (2.20)-(2.22) simultaneously, to be able to handle the ghost points which occur in the resulting finite difference equations.

The boundary conditions at $x = 0$ and $x = \sqrt{2}$ are given in Equation (3.6) and Equation (3.8), respectively. Applying second and fourth order approximation formulas (2.14)-(2.20) to $\partial u/\partial x$ at $x = 0$ and $x = \sqrt{2}$, we obtain

$$U_{-1,j} = 2h\rho\lambda U_{0,j} + U_{1,j}, \qquad U_{N+1,j} = 2h\rho\lambda U_{N,j} + U_{N-1,j}, \tag{3.20}$$

$$U_{-2,j} = 4h\rho\lambda U_{0,j} + U_{2,j}, \qquad U_{N+2,j} = 4h\rho\lambda U_{N,j} + U_{N-2,j} \tag{3.21}$$

in which the ghost points $U_{-1,j}$, $U_{-2,j}$, $U_{N+1,j}$ and $U_{N+2,j}$ are written in terms of the grid points inside the domain Ω. Similarly, with the use of second and fourth order central difference formulas (2.15)-(2.22) to approximate $\partial u/\partial y$ in boundary conditions given in (3.6)-(3.8) along $y = 0$ and $y = \sqrt{2}$, we obtain

$$U_{i,-1} = 2h\rho\lambda U_{i,0} + U_{i,1}, \qquad U_{i,N+1} = 2h\rho\lambda U_{i,N} + U_{i,N-1}, \tag{3.22}$$

$$U_{i,-2} = 4h\rho\lambda U_{i,0} + U_{i,2}, \qquad U_{i,N+2} = 4h\rho\lambda U_{i,N} + U_{i,N-2}. \tag{3.23}$$

Once the difference equation (3.19) is written for $i, j = 0, 1, \cdots, N$ the arising ghost points in the linear system are removed by using the equations (3.20)-(3.23). Thus, the final system will be of size $(N + 1) \times (N + 1)$ which is given in the following generalized eigenvalue problem

$$AU = \tilde{\lambda} BU \tag{3.24}$$

with $\tilde{\lambda} = h\rho\lambda$. Here, U is the unknown vector taken in the following order:

$$U^T = \Big[U_{0,0} \;\; U_{1,0} \;\; \cdots \;\; U_{N,0} \;\; | \;\; U_{0,1} \;\; U_{1,1} \;\; \cdots \;\; U_{N,1} \;\; | \;\; \cdots \;\; | \;\; U_{0,N} \;\; U_{1,N} \;\; \cdots \;\; U_{N,N}\Big]. \quad (3.25)$$

The matrix A is constructed by the matrices C, D and the identity matrix I of size $(N+1) \times (N+1)$, and they have the following forms:

$$A = \begin{bmatrix}
C & 32I & -2I & 0 & \cdots & & & & 0 \\
16I & D & 16I & -I & & & & & \\
-I & 16I & C & 16I & -I & & & & \\
0 & -I & 16I & C & 16I & & & & \\
\vdots & & & & & & & & 0 \\
 & & & & & & C & 16I & -I \\
 & & & & & 0 & -I & 16I & D & 16I \\
0 & \cdots & & & & 0 & 0 & -2I & 32I & C
\end{bmatrix},$$

$$C = \begin{bmatrix}
k_1 & 32 & -2 & 0 & \cdots & & & & 0 \\
16 & k_1 - 1 & 16 & -1 & & & & & \\
-1 & 16 & k_1 & 16 & -1 & & & & \\
0 & -1 & 16 & k_1 & 16 & & & & \\
\vdots & & & & & & & & 0 \\
 & & & & & & k_1 & 16 & -1 \\
 & & & & & 0 & -1 & 16 & k_1 - 1 & 16 \\
0 & \cdots & & & & 0 & 0 & -2 & 32 & k_1
\end{bmatrix},$$

$$D = \begin{bmatrix} k_2 & 32 & -2 & 0 & & & & & & 0 \\ 16 & k_2-1 & 16 & -1 & & & & & & \\ -1 & 16 & k_2 & 16 & -1 & & & & & \\ 0 & -1 & 16 & k_2 & 16 & & & & & \\ & & & & & & & & & 0 \\ & & & & & & & k_2 & 16 & -1 \\ & & & & & 0 & -1 & 16 & k_2-1 & 16 \\ 0 & & & & & 0 & 0 & -2 & 32 & k_2 \end{bmatrix},$$

where $k_1 = k_2 + 1 = -60 - 12\mu h^2$. On the other hand, B has the form

$$B = \begin{bmatrix} E & 0 & 0 & & & 0 \\ 2I & F & 0 & & & \\ 0 & 0 & & & & \\ & & & & & 0 \\ & & & & F & 2I \\ 0 & & & 0 & 0 & E \end{bmatrix},$$

where

$$E = \begin{bmatrix} -56 & 0 & 0 & & & 0 \\ 2 & -28 & 0 & & & \\ 0 & 0 & & & & \\ & & & & & 0 \\ & & & & -28 & 2 \\ 0 & & & 0 & 0 & -56 \end{bmatrix}, \quad F = \begin{bmatrix} -28 & 0 & 0 & & & 0 \\ 2 & 0 & 0 & & & \\ 0 & 0 & & & & \\ & & & & & 0 \\ & & & & 0 & 2 \\ 0 & & & 0 & 0 & -28 \end{bmatrix}$$

are the matrices of size $(N+1) \times (N+1)$.

Table 3.7 and Table 3.8 contain the smallest ten approximate eigenvalues λ_i^h for varying number of subintervals up to $N = 1500$ and reference eigenvalues λ_i of the standard Steklov EVP with $\mu = 4$ and $\mu = -4 - 4i$, respectively, and $\rho = -1$. The reference values λ_i given in the second column's of Tables 3.7 and 3.8 are chosen from the approximate values obtained by using $N = 2048$ grid points for both values

Table 3.7: Eigenvalues of Steklov EVP by $O_4B_{2,4}$ for $\mu = -4$ and $\rho = -1$.

i	Ref. (λ_i)	$N = 256$	$N = 512$	$N = 1024$
1	-0.21225215	-0.21225070	-0.21225180	-0.21225208
2	-0.21225215	-0.21225070	-0.21225180	-0.21225208
3	-0.90805601	-0.90805146	-0.90805493	-0.90805580
4	2.20250695	2.20249594	2.20250433	2.20250643
5	-2.76894717	-2.76896256	-2.76895083	-2.76894790
6	-2.76894717	-2.76896256	-2.76895083	-2.76894790
7	-2.91855138	-2.91857370	-2.91855669	-2.91855245
8	-2.91855138	-2.91857370	-2.91855669	-2.91855245
9	-5.22710385	-5.22735338	-5.22716316	-5.22711570
10	-5.22710385	-5.22735338	-5.22716316	-5.22711570

of $\mu = -4$ and $\mu = -4 - 4i$. Even for the smallest value of N, it can be seen that the approximate results are sufficiently close to the reference values, and at least five digits accuracy is obtained.

Table 3.8: Eigenvalues of Steklov EVP by $O_4B_{2,4}$ for $\mu = -4 - 4i$ and $\rho = -1$.

i	Ref. (λ_i)	$N = 500$	$N = 1000$	$N = 1500$
1	-0.343046 +0.850746i	-0.343045 +0.850746i	-0.343046 +0.850746i	-0.343046+ 0.850746i
2	-0.343046 +0.850746i	-0.343045 +0.850746i	-0.343046 +0.850746i	-0.343046+ 0.850746i
3	-0.950110 +0.540097i	-0.950108 +0.540097i	-0.950110 +0.540097i	-0.950110+ 0.540097i
4	0.686552 +2.495294i	0.686554 +2.495290i	0.686552 +2.495293i	0.686552+ 2.495294i
5	-2.796524 +0.540730i	-2.796527 +0.540738i	-2.796525 +0.540732i	-2.796524+ 0.540731i
6	-2.796524 +0.540730i	-2.796527 +0.540738i	-2.796525 +0.540732i	-2.796524+ 0.540731i
7	-2.931161 +0.474173i	-2.931166 +0.474181i	-2.931162 +0.474175i	-2.931161+ 0.474174i
8	-2.931161 +0.474173i	-2.931166 +0.474181i	-2.931162 +0.474175i	-2.931161+ 0.474174i
9	-5.234827 +0.329777i	-5.234889 +0.329794i	-5.234840 +0.329780i	-5.234831+ 0.329778i
10	-5.234827 +0.329777i	-5.234889 +0.329794i	-5.234840 +0.329780i	-5.234831+ 0.329778i

Figure 3.8 and Figure 3.9 display the normalized errors ε_i of λ_i found by fourth order central difference formula in log-log scale respectively for $\mu = -4$ and $\mu = -4 - 4i$. For both values of μ, these figures show that the approximate eigenvalue λ_i^h has a

convergence behavior of order $O(h^2)$ to the approximate reference values.

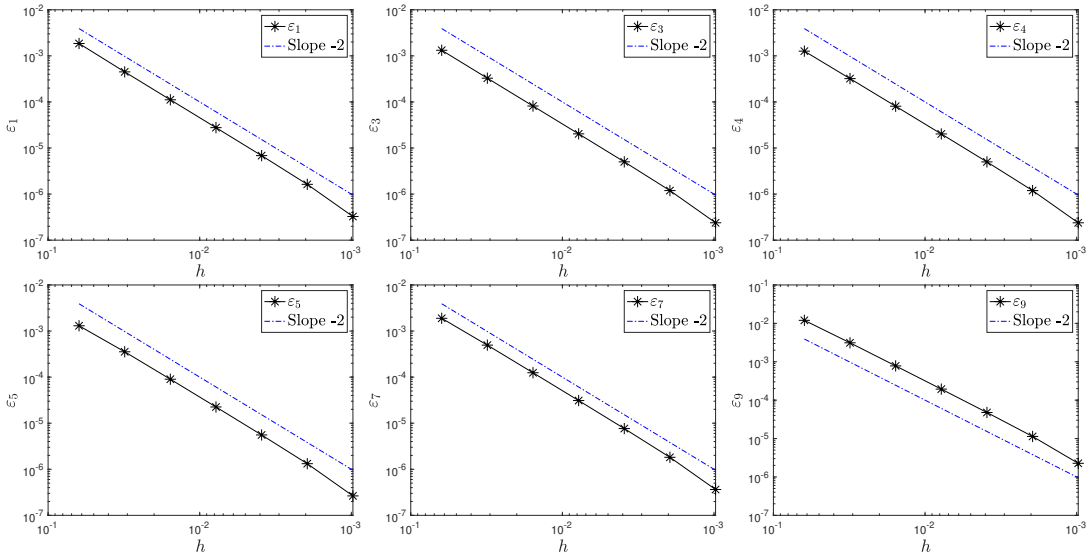

Figure 3.8: Convergence behavior of λ_i^h to λ_i versus the step size h in log-log scale for $\mu = -4$ and $\rho = -1$ by $O_4B_{2,4}$.

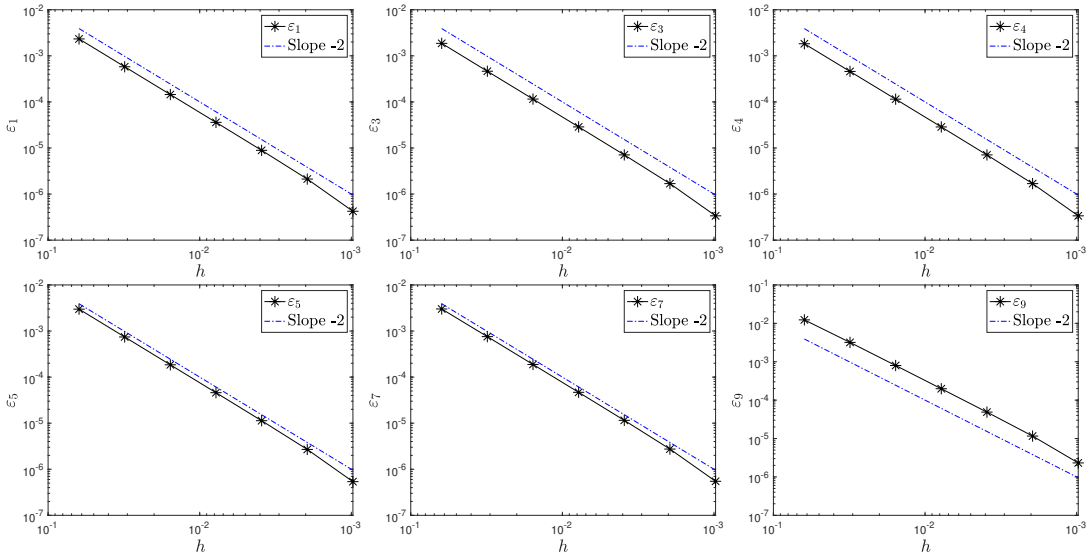

Figure 3.9: Convergence behavior of λ_i^h to λ_i versus the step size h in log-log scale for $\mu = -4 - 4i$ and $\rho = -1$ by $O_2B_{2,4}$.

Moreover, Figure 3.10 shows the contour plots of the eigenfunctions U_1,U_3,U_4,U_5,U_7 and U_9 of Steklov EVP corresponding to the eigenvalues λ_1, λ_3,λ_4,λ_5 λ_7 and λ_9.

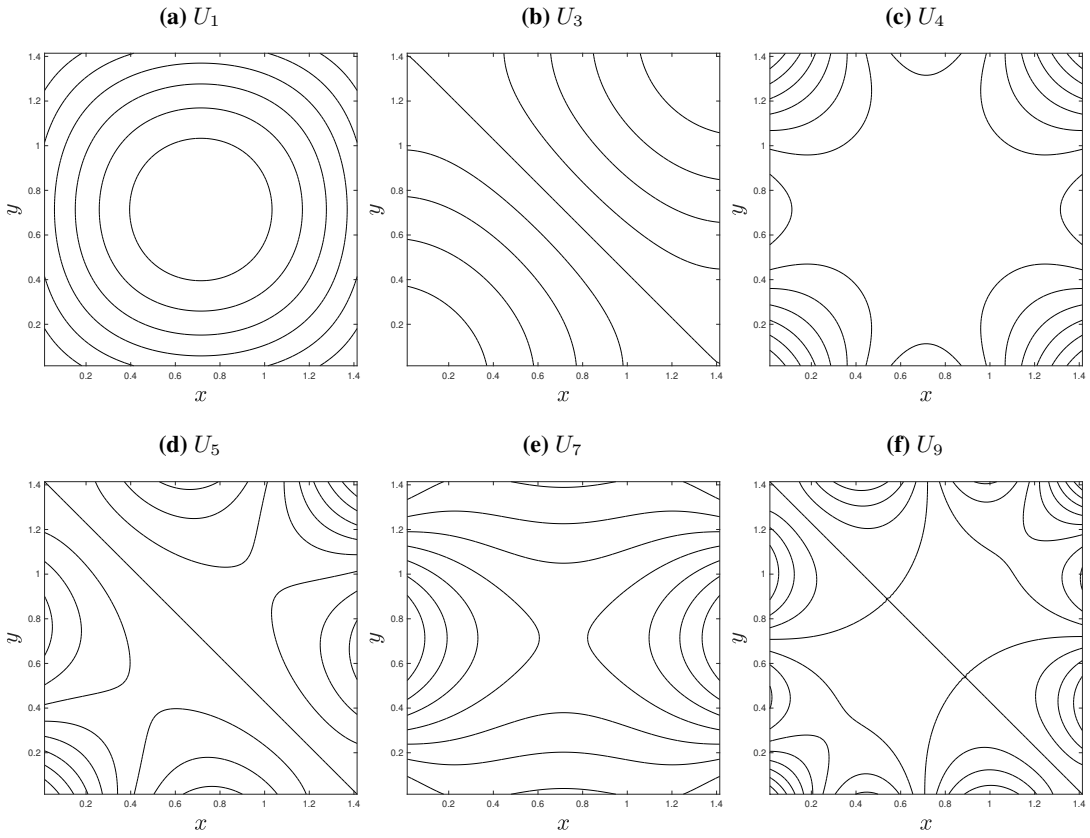

Figure 3.10: Eigenfunctions corresponding to the eigenvalues λ_i, $i = 1, 3, 4, 5, 7, 9$ of Steklov EVP with $\mu = -4$ and $\rho = -1$.

In conclusion, the relationship between the convergence order and the order of the method used in the approximation of the boundary conditions where the eigenvalues lie, is a significant aspect that we highlight. When the second order approximation to the differential equation and the first order approximations forward and backward differences to boundary conditions are applied, a first order, that is $O(h)$ convergence rate of the approximate eigenvalues λ_i^h to the reference values λ_i is obtained. Moreover, the convergence order is advanced to second order ($O(h^2)$) when the boundary conditions are approximated by the second order central difference approximations. On the other hand, approximation of the differential equations either by the second or fourth order central difference FDM results in a same convergence rate of order $O(h^2)$. The reason not observing an increase in the convergence rate by the use of fourth order finite differences could be the result of using a second order finite difference in the discretization of the boundary conditions to be able to handle the ghost points.

3.2 A Mixed Type Steklov Eigenvalue Problem

In this section, a mixed type Steklov EVP, in which the boundary $\partial\Omega = \Gamma_\lambda \cup \Gamma_N$ is divided into two parts with different boundary conditions, is examined by using fourth order finite difference formulas to discretize the differential equation since when a second order difference formula is applied an almost linear convergence is obtained as shown in parenthesis at the last column of Table 3.9.

Table 3.9: Eigenvalues of mixed Steklov EVP by O_2B_2.

Ref	$N = 128$	$N = 256$	$N = 512$	$N = 1024$
0	2.778613735e-12	1.281139203e-11	5.543178875e-11	2.175425979e-10(-)
3.129881036	3.115810130	3.122909788	3.126411468	3.128150266 (1.00)
6.283141484	6.177289147	6.230393086	6.256813408	6.269989185 (1.00)
9.424777838	9.151039252	9.287981836	9.356407359	9.390600633 (1.00)
12.566370614	12.049532500	12.307415896	12.436787838	12.501556487 (0.99)
15.707963268	14.873926699	15.288996603	15.498059832	15.602915122 (0.99)
18.849555922	17.625372758	18.232987910	18.540286113	18.694691891 (0.99)
21.991148575	20.305052994	21.139658542	21.563530003	21.776902110 (0.99)
25.132741229	22.914178021	24.009281913	24.567855480	24.849561184 (0.99)
28.274333882	25.453983555	26.842135928	27.553327167	27.912684603 (0.99)

The mixed type Steklov EVP differs from the standard Steklov EVP in terms of the taken boundary conditions. In the standard Steklov EVP, on the whole boundary the mixed type boundary conditions with the spectral parameter λ is taken whereas in the mixed type Steklov EVP, the boundary is divided into two parts such that on the part Γ_λ the mixed type boundary condition is taken and on the part Γ_N the Neumann type boundary condition is taken. Specifically, Steklov EVP in Equation (3.1) is considered on the domain $\Omega = [0,1] \times [0,1]$ with $\rho = 1$ and $\mu = 0$, and it has the form

$$\begin{cases} \Delta u = 0 & \text{in } \Omega, \\ \partial u/\partial n = \lambda u & \text{on } \Gamma_\lambda, \\ \partial u/\partial n = 0 & \text{on } \Gamma_N, \end{cases} \tag{3.26}$$

with the boundary $\partial\Omega = \Gamma_\lambda \cup \Gamma_N$ where $\Gamma_\lambda = \{(x,y) \mid 0 \leq x \leq 1, y = 1\}$,

$\Gamma_N = \partial\Omega \setminus \Gamma_\lambda$, since this problem has exact the eigensolutions that are given in [23] as follows:

$$u_i(x,y) = \cos(i\pi x)\cosh(i\pi y), \quad \lambda_i = i\pi \tanh(i\pi),\ i \in \mathbb{N}. \tag{3.27}$$

The discretization of the Laplace equation in Equation (3.26) is performed by the use of fourth order formulas (2.21)-(2.23) at an interior node (x_i, y_j), with N equal lengths of subintervals in x and y-directions, i.e. $h = k = 1/N$. Thus, the following difference equation

$$\begin{aligned}\frac{1}{12h^2}(-U_{i+2,j} + 16U_{i+1,j} - 30U_{i,j} + 16U_{i-1,j} - U_{i-2,j}) + \frac{1}{12h^2}(-U_{i,j+2} + 16U_{i,j+1} \\ -30U_{i,j} + 16U_{i,j-1} - U_{i,j-2}) = 0,\end{aligned} \tag{3.28}$$

is obtained for the Laplace equation which can be rewritten as:

$$\begin{aligned}-U_{i+2,j} + 16U_{i+1,j} - 60U_{i,j} + 16U_{i-1,j} - U_{i-2,j} - U_{i,j+2} \\ +16U_{i,j+2} + 16U_{i,j-1} - U_{i,j-2} = 0.\end{aligned} \tag{3.29}$$

On the other hand, the boundary conditions are approximated either by using first order backward and forward differences and second order central differences in Section 3.2.a; and by using second and fourth order central differences in Section 3.2.b as in the previous Section 3.1 for the standard Steklov EVP.

3.2.a Approximation of the Boundary Conditions by Central-Backward and Central-Forward Difference Formulas $(O_4B_{1,2})$

The boundary condition is discretized in this section using the forward difference formulas (2.7)-(2.8), the backward difference formulas (2.11)-(2.12) and the central difference formulas (2.14)-(2.15).

The boundary conditions at $x = 0$ and $y = 0$ are

$$\frac{\partial u}{\partial n} = -\frac{\partial u}{\partial x} = 0 \quad \text{and} \quad \frac{\partial u}{\partial n} = -\frac{\partial u}{\partial y} = 0. \tag{3.30}$$

Applying the central difference formulas (2.14)-(2.15) and forward difference formulas (2.7)-(2.8) to the first partial derivative $\partial u/\partial x$ at $x = 0$ and to $\partial u/\partial x$ at $y = 0$

respectively, we obtain

$$U_{-1,j} = U_{1,j}, \quad U_{0,j} = U_{1,j}, \tag{3.31}$$

$$U_{i,-1} = U_{i,1}, \quad U_{i,0} = U_{i,1}. \tag{3.32}$$

The boundary conditions at $x = 1$ and $y = 1$ are

$$\frac{\partial u}{\partial n} = \frac{\partial u}{\partial x} = 0 \quad \text{and} \quad \frac{\partial u}{\partial n} = \frac{\partial u}{\partial y} = \lambda u. \tag{3.33}$$

Approximating $\partial u/\partial x$ and $\partial u/\partial y$ at $x = 1$ and $y = 1$ by the central difference formulas (2.14)-(2.15) and backward difference formulas (2.11)-(2.12) results in,

$$U_{N+1,j} = U_{N-1,j}, \qquad U_{N,j} = U_{N-1,j}, \tag{3.34}$$

$$U_{i,N+1} = 2h\lambda U_{i,N} + U_{i,N-1}, \qquad U_{i,N} = U_{i,N-1} + h\lambda U_{i,N}. \tag{3.35}$$

Inserting these boundary conditions into the difference equation (3.29) yields $(N+1)^2$ linear equations which can be written in the matrix form:

$$AU = \tilde{\lambda} BU \tag{3.36}$$

which is the generalized eigenvalue problem with $\tilde{\lambda} = h\lambda$. Here, U is the unknown vector having the form

$$U^T = \Big[U_{0,0} \;\; U_{1,0} \;\; \cdots \;\; U_{N,0} \;\; | \;\; U_{0,1} \;\; U_{1,1} \;\; \cdots \;\; U_{N,1} \;\; | \;\; \cdots \;\; | \;\; U_{0,N} \;\; U_{1,N} \;\; \cdots \;\; U_{N,N}\Big]. \tag{3.37}$$

The matrix A is in the form

$$A = \begin{bmatrix}
C & 16I & -I & 0 & & & & & 0 \\
15I & D & 16I & -I & & & & & \\
-I & 16I & D & 16I & -I & & & & \\
0 & -I & 16I & D & 16I & & & & \\
 & & & & & \ddots & & & 0 \\
 & & & & & & D & 16I & -I \\
 & & & & 0 & -I & 16I & E & 16I \\
0 & & & & 0 & 0 & 0 & -I & I
\end{bmatrix},$$

where the matrices C, D and E are of size $(N+1) \times (N+1)$ and have the forms

$$C = \begin{bmatrix} -30 & 16 & -1 & 0 & \cdots & & & & 0 \\ 15 & -45 & 16 & -1 & & & & & \\ -1 & 16 & -45 & 16 & -1 & & & & \\ 0 & -1 & 16 & -45 & 16 & & & & \\ \vdots & & & & & & & & \\ & & & & & & & & 0 \\ & & & & & & -45 & 16 & -1 \\ & & & & & 0 & -1 & 16 & 15 \\ 0 & \cdots & & & & 0 & 0 & -1 & 16 & -30 \end{bmatrix},$$

$$D = \begin{bmatrix} -45 & 32 & -1 & 0 & \cdots & & & & 0 \\ 15 & -60 & 16 & -1 & & & & & \\ -1 & 16 & -60 & 16 & -1 & & & & \\ 0 & -1 & 16 & -60 & 16 & & & & \\ \vdots & & & & & & & & \\ & & & & & & & & 0 \\ & & & & & & -60 & 16 & -1 \\ & & & & & 0 & -1 & 16 & 15 \\ 0 & \cdots & & & & 0 & 0 & -1 & 16 & -45 \end{bmatrix},$$

$$E = \begin{bmatrix} -46 & 32 & -1 & 0 & \cdots & & & & 0 \\ 15 & -61 & 16 & -1 & & & & & \\ -1 & 16 & -61 & 16 & -1 & & & & \\ 0 & -1 & 16 & -61 & 16 & & & & \\ \vdots & & & & & & & & \\ & & & & & & & & 0 \\ & & & & & & -61 & 16 & -1 \\ & & & & & 0 & -1 & 16 & 15 \\ 0 & \cdots & & & & 0 & 0 & -1 & 16 & -46 \end{bmatrix}.$$

On the other hand, the matrix B on the right hand side of Equation (3.36) has the form

$$B = \begin{bmatrix} 0 & 0 & 0 & \cdots & 0 \\ 0 & 0 & 0 & \iddots & \vdots \\ 0 & 0 & \iddots & \iddots & 0 \\ \vdots & \iddots & \iddots & 0 & 2I \\ 0 & \cdots & 0 & 0 & I \end{bmatrix},$$

where the identity matrix I is of size $(N+1) \times (N+1)$.

After the generalized eigenvalue problem (3.36) is solved, the results are obtained as given in Table 3.10. This table contains the smallest ten exact eigenvalues λ_i and approximate eigenvalues λ_i^h for the values of N =256, 512 and 1024. Using more grid points yields better approximations λ_i^h to the exact eigenvalues λ_i especially for smaller eigenvalues.

Table 3.10: Eigenvalues of mixed Steklov EVP by $O_4B_{1,2}$.

i	λ_i	$N = 128$	$N = 256$	$N = 512$	$N = 1024$
1	0	-5.336e-13	-2.973e-12	-1.219e-11	-4.237e-11
2	3.129881	3.113851	3.121891	3.125889	3.127886
3	6.283141	6.162811	6.222714	6.252861	6.267985
4	9.424778	9.115316	9.268541	9.346236	9.385422
5	12.566371	11.985315	12.271639	12.417783	12.491793
6	15.707963	14.775431	15.232486	15.467700	15.587186
7	18.849556	17.488095	18.152431	18.496088	18.671645
8	21.991149	20.125623	21.029232	21.503164	21.745215
9	25.132741	22.690335	23.867428	24.489011	24.807929
10	28.274334	25.184437	26.666480	27.453817	27.859842

Figure 3.11 illustrates the convergence behaviour of the normalized error ε_i for the corresponding eigenvalues λ_i, $i = 2, 3, 4, 6, 8, 10$. This figure shows that as in the standard Steklov EVP, the convergence rate of the approximate eigenvalues to the exact ones is of order $O(h)$ in the mixed Steklov EVP when central-forward and

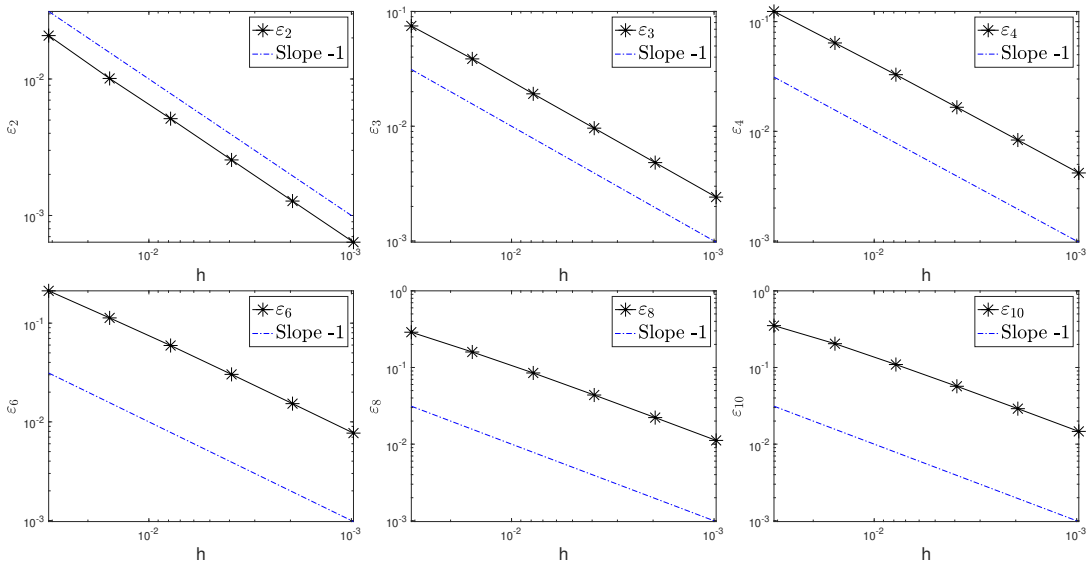

Figure 3.11: Convergence behavior of λ_i^h to λ_i versus the step size h in log-log scale by $O_4B_{1,2}$.

central-backward differences are applied to the given boundary conditions.

3.2.b Approximation of the Boundary Condition by Second and Fourth Order Central Difference Formulas $(O_4B_{2,4})$

In this section, the mixed and Neumann type boundary conditions are discretized by the second order central difference formulas (2.14)-(2.15) and the fourth order central difference formulas (2.20)-(2.22). That is, the boundary conditions at $x = 0$ and $x = 1$ given in Equation (3.30) and Equation (3.33) are discretized by the second and fourth order central difference formulas (2.14) and (2.20), and we obtain

$$U_{-1,j} = U_{1,j}, \qquad U_{-2,j} = U_{2,j}, \tag{3.38}$$

$$U_{N+1,j} = U_{N-1,j}, \quad U_{N+2,j} = U_{N-2,j}. \tag{3.39}$$

Similarly, the boundary conditions at $y = 0$ and $y = 1$ given in Equation (3.30) and Equation (3.33) are discretized by the second and fourth order central difference formulas (2.15) and (2.22), which results in

$$U_{i,-1} = U_{i,1}, \qquad U_{i,-2} = U_{i,2}, \tag{3.40}$$

$$U_{i,N+1} = 2h\lambda U_{i,N} + U_{i,N-1}, \quad U_{i,N+2} = 4h\lambda U_{i,N} + U_{i,N-2}. \tag{3.41}$$

Inserting these boundary conditions into the difference equation (3.29) yields $(N+1)^2$ linear equations which can be written in the following generalized EVP

$$AU = \tilde{\lambda} BU \tag{3.42}$$

with $\tilde{\lambda} = h\lambda$ and the vector U is ordered as follows:

$$U^T = \Big[U_{0,0} \;\; U_{1,0} \;\; \cdots \;\; U_{N,0} \;\; | \;\; U_{0,1} \;\; U_{1,1} \;\; \cdots \;\; U_{N,1} \;\; | \;\; \cdots \;\; | \;\; U_{0,N} \;\; U_{1,N} \;\; \cdots \;\; U_{N,N}\Big]. \tag{3.43}$$

The matrix A is formed by C and D matrices of sizes $(N+1)\times(N+1)$ as follows:

$$A = \begin{bmatrix}
C & 32I & -2I & 0 & & & & & 0 \\
16I & D & 16I & -I & & & & & \\
-I & 16I & D & 16I & -I & & & & \\
0 & -I & 16I & D & 16I & & & & \\
 & & & & & \ddots & & & \\
 & & & & & & D & 16I & -I \\
 & & & & 0 & -I & 16I & D & 16I \\
0 & & & & 0 & 0 & -2I & 32I & D
\end{bmatrix},$$

$$C = \begin{bmatrix}
-60 & 32 & -2 & 0 & & & & & 0 \\
16 & -61 & 16 & -1 & & & & & \\
-1 & 16 & -60 & 16 & -1 & & & & \\
0 & -1 & 16 & -60 & 16 & & & & \\
 & & & & & \ddots & & & \\
 & & & & & & -60 & 16 & -1 \\
 & & & & 0 & -1 & 16 & -61 & 16 \\
0 & & & & 0 & 0 & -2 & 32 & -60
\end{bmatrix},$$

$$D = \begin{bmatrix} -61 & 32 & -2 & 0 & \cdots & \cdots & \cdots & 0 \\ 16 & -62 & 16 & -1 & \ddots & & & \vdots \\ -1 & 16 & -61 & 16 & -1 & \ddots & & \\ 0 & -1 & 16 & -61 & 16 & \ddots & \ddots & \\ \vdots & \ddots & \ddots & \ddots & \ddots & \ddots & 0 & \\ & & & & & -61 & 16 & -1 \\ & & & 0 & -1 & 16 & -62 & 16 \\ 0 & \cdots & \cdots & 0 & 0 & -2 & 32 & -61 \end{bmatrix}.$$

On the other hand, the matrix B is in the form:

$$B = \begin{bmatrix} 0 & 0 & 0 & \cdots & \cdots & 0 \\ 0 & 0 & 0 & \ddots & & \vdots \\ 0 & 0 & \ddots & \ddots & & \\ \vdots & \ddots & \ddots & \ddots & 0 & \\ & & & 0 & 2I \\ 0 & \cdots & \cdots & 0 & 0 & -28I \end{bmatrix}$$

where the identity matrix I is of size $(N+1) \times (N+1)$.

In Table 3.11, the approximate and exact smallest ten eigenvalues of the mixed Steklov EVP are presented for the values of $N = 256, 512, 1024$. It is well observed that using higher order central difference formulas gives better accuracy in obtaining eigenvalues when compared with the results in Table 3.10 obtained by the first order finite difference formulas.

Table 3.11: Eigenvalues of the mixed type Steklov EVP by $O_4B_{2,4}$.

i	Ref.	$N = 256$	$N = 512$	$N = 1024$
1	0.0000	-2.974e-12	-1.077e-11	-4.739e-11
2	3.129881	3.129920	3.129891	3.129883
3	6.283141	6.283458	6.283220	6.283161
4	9.424778	9.425848	9.425045	9.424844
5	12.566371	12.568910	12.567004	12.566529
6	15.707963	15.712931	15.709201	15.708272
7	18.849556	18.858152	18.851696	18.850090
8	21.991149	22.004817	21.994549	21.991996
9	25.132741	25.153170	25.137821	25.134007
10	28.274334	28.303455	28.281572	28.276137

This result is also certified by Figure 3.12, which shows a second order convergence rate of the approximate eigenvalues λ_i^h, $i = 2, 3, \cdots, 10$, to the exact ones. That is, the relative error variation with respect to step size h is parallel to a line with slope $m = -2$. The same convergence behavior was also obtained in the case of standard eigenvalue problem given in Section 3.1.b.

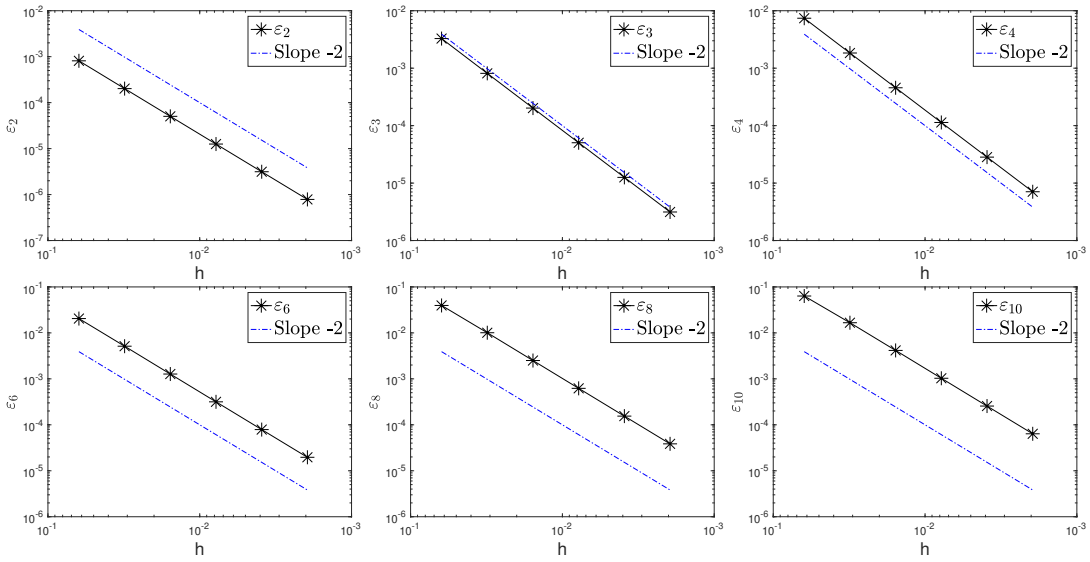

Figure 3.12: Convergence behavior of λ_i^h to λ_i versus the step size h in log-log scale by $O_4B_{2,4}$.

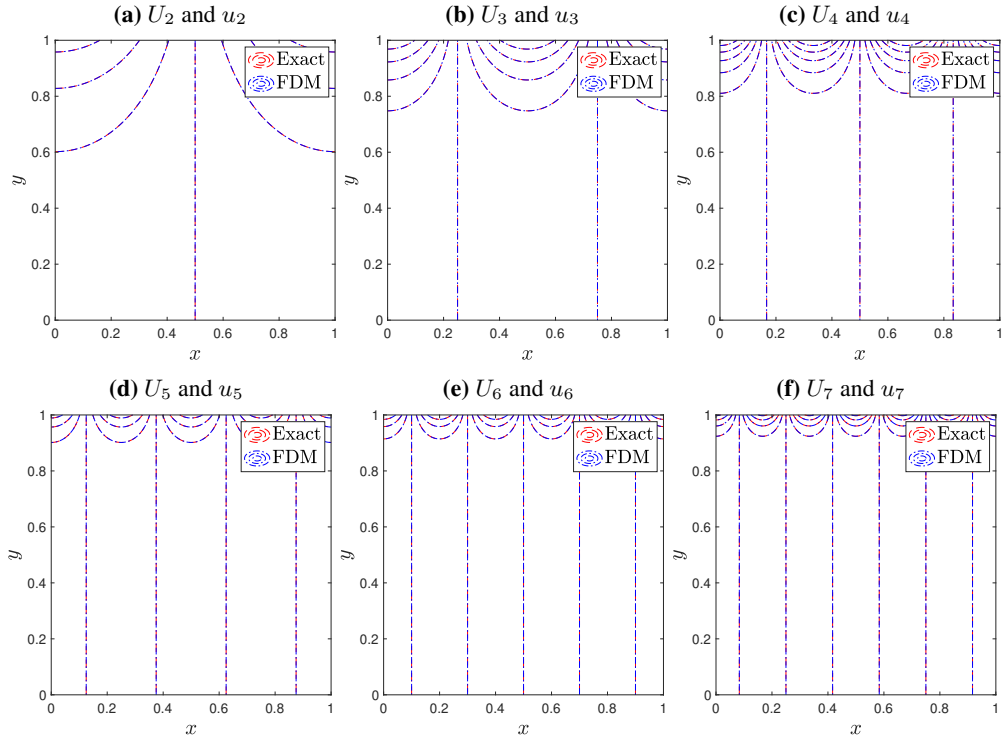

Figure 3.13: Plot of the eigenfunctions of the mixed type Steklov EVP.

Finally, contour plots of the eigenfunctions corresponding to the eigenvalues λ_2,λ_3, λ_4, λ_5, λ_6, λ_7 and λ_8 are displayed in Figure 3.13. As observed in Table 3.11 all eigenvalues of mixed Steklov EVP are simple so that all correspond to only one linearly independent eigenfunction. Thus, no matching issues between the exact and approximate eigenfunctions observed in the simplified Steklov EVP in Section 3.1, is encountered here in the contour plots. That is, the approximate eigenfunctions U_i agrees very well with the exact eigenfunctions u_i, $i = 2, 3, 4, 5, 6, 7$.

To conclude, the present chapter is devoted for the approximate solutions to the Steklov EVPs by using finite difference approaches of different orders especially for the discretization of the boundary conditions. It is seen that approximating only the differential equation with higher order finite differences (in this chapter fourth order instead of second order) has no effect in the advancement of convergence behavior of approximate eigenvalues. However, the convergence rate becomes faster when both the differential equation and the boundary conditions are approximated by using higher order finite difference formulas of at least second order. That is, the conver-

gence rate is advanced from first order (i.e. $O(h)$) to second order (i.e. $O(h^2)$) by combining a fourth order FDM in approximating the differential equation with a second and fourth order central differences applied to the boundary conditions as shown in Table 3.12.

Table 3.12: Convergence rates for standard and mixed type Steklov EVPs.

	Standard Steklov EVP			Mixed type Steklov EVP		
Order of method	O_2B_1	O_2B_2	$O_4B_{2,4}$	O_2B_2	$O_4B_{1,2}$	$O_4B_{2,4}$
Convergence rate of eigenvalues	$O(h)$	$O(h^2)$	$O(h^2)$	$O(h)$	$O(h)$	$O(h^2)$

To the best of author's knowledge, the solution of mixed type Steklov EVP by FDM is not available in the literature. In this sense, this chapter can be considered as one of the main contribution of the present thesis to the field on the numerical solutions of the Steklov eigenvalue problems. Moreover, FDM can be thought as an effective numerical approach for the solution of Steklov EVPs since it is easy to implement and yields a second order convergence.

CHAPTER 4

CONCLUSION

This thesis provides the second and fourth order FDM approximations of Poisson problem, Laplace EVP and Steklov EVPs on square domains. The convergence behavior of the finite difference solutions to the exact ones is investigated in both of the Poisson problem and the Laplace EVP. It is found that our computer codes have performed correctly and efficiently with the FDM. When the second order method is used to approximate the Laplace operator in the equation of Laplace EVP, the eigenvalues have a quadratic convergence behavior, however, when the fourth order method is employed, a fourth order convergence is well observed. Additionally, it is determined that the linear combinations of the linearly independent approximate eigenfunctions of the Laplace EVP corresponding to the double eigenvalues in the two-dimensional case give reasonably well approximations to the related exact eigenfunctions.

On the other hand, we take into account two Steklov eigenproblems that differ from one another due to the corresponding boundary conditions. The first one has the well-known form which we called the standard Steklov EVP. This problem is considered on square domains, specifically on $\Omega = [-1, 1] \times [-1, 1]$ where the analytical solution exists [11], and on $\Omega = [0, \sqrt{2}] \times [0, \sqrt{2}]$ with no analytical solution. If the analytical solution is available, it is utilized as a reference value to examine the convergence behavior of the approximated eigenvalues, and to verify its agreement with the approximate eigenfunctions. In the absence of analytical solutions, the best approximations (those produced with the largest N value) are used. It has been found that using the fourth order method only for the Laplace operator and second order method for the boundary conditions has no advancing effect on the convergence rate of the eigenvalues. On the other hand, the convergence behavior of the approximate

eigenvalues is improved by using higher order difference formulas to the boundary conditions as well. Thus, a quadratic convergence behavior is obtained for the eigenvalues of the standard Steklov EVP.

Finally, the mixed type Steklov EVP [23] is considered on square domain $\Omega = [0,1] \times [0,1]$ with the Neumann and spectral parameter type boundary conditions on some part of the boundary of the computational domain. Fourth order FDM is used to investigate eigensolutions, and formulas of various orders are used to discretize the boundary conditions. Analytical solutions are taken as the reference values to analyze the convergence behavior of the eigenvalues. All the results for eigenfunctions obtained from the numerical experiments, have been proven to be in well coherence with the experimental and theoretical findings.

The presented numerical results have also revealed the fact that the FDM is an efficient numerical approach for the solutions of Steklov EVPs, and it is simple to implement in order to produce a reasonably well convergence rate of eigenvalues.

The present study can be thought as a basic analysis of the Steklov EVP by using FDM. It can be extended for the FDM solutions of Steklov type eigenvalue problems defined in more complex computational domains, e.g. circular and cuspidal domains. Moreover, the effect of the application of a combination of different finite difference formulas to the differential equation and the boundary conditions can be considered as well with a discussion of the convergence of the method.

REFERENCES

[1] M. Kline and P. Kline, *Mathematical Thought from Ancient to Modern Times*. Oxford paperbacks, Oxford University Press, 1972.

[2] H. T. Betteridge, "New Cassell's German dictionary; German-English English-German," 1965.

[3] T. Hawkins, "Cauchy and the spectral theory of matrices," *Historia Mathematica*, vol. 2, no. 1, pp. 1–29, 1975.

[4] N. Kuznetsov, T. Kulczycki, M. Kwaśnicki, A. Nazarov, S. Poborchi, I. Polterovich, and B. o. Siudeja, "The legacy of Vladimir Andreevich Steklov," *Notices of the American Mathematical Society*, vol. 61, no. 1, pp. 9–22, 2014.

[5] J. Planchard and B. Thomas, "On the dynamical stability of cylinders placed in cross-flow," *Journal of Fluids and Structures*, vol. 7, no. 4, pp. 321–339, 1993.

[6] J. Canavati and A. A. Minzoni, "A discontinuous Steklov problem with an application to water waves," *Journal of Mathematical Analysis and Applications*, vol. 69, no. 2, pp. 540–558, 1979.

[7] Y. Saad, J. R. Chelikowsky, and S. M. Shontz, "Numerical methods for electronic structure calculations of materials," *SIAM Review*, vol. 52, no. 1, pp. 3–54, 2010.

[8] H. C. Mayer and R. Krechetnikov, "Walking with coffee: Why does it spill?," *Physical Review E*, vol. 85, no. 4, p. 046117, 2012.

[9] G. Uhlmann, "Inverse problems: seeing the unseen," *Bulletin of Mathematical Sciences*, vol. 4, no. 2, pp. 209–279, 2014.

[10] P. Kuchment, "The mathematics of photonic crystals," in *Mathematical Modeling in Optical Science*, pp. 207–272, SIAM, 2001.

[11] A. Girouard and I. Polterovich, "Spectral geometry of the steklov problem (survey article)," *Journal of Spectral Theory*, vol. 7, no. 2, pp. 321–359, 2017.

[12] B. Ghojogh, F. Karray, and M. Crowley, "Eigenvalue and generalized eigenvalue problems: Tutorial," *arXiv preprint arXiv:1903.11240*, 2019.

[13] M. Nool and A. van der Ploeg, "A parallel Jacobi-Davidson-type method for solving large generalized eigenvalue problems in magnetohydrodynamics," *SIAM Journal on Scientific Computing*, vol. 22, no. 1, pp. 95–112, 2000.

[14] D. S. Grebenkov and B.-T. Nguyen, "Geometrical structure of Laplacian eigenfunctions," *SIAM Review*, vol. 55, no. 4, pp. 601–667, 2013.

[15] O. Steinbach and G. Unger, "A boundary element method for the Dirichlet eigenvalue problem of the Laplace operator," *Numerische Mathematik*, vol. 113, no. 2, pp. 281–298, 2009.

[16] H. P. W. Gottlieb, "Eigenvalues of the Laplacian with Neumann boundary conditions," *Australian Mathematical Society. Journal. Series B. Applied Mathematics*, vol. 26, no. 3, pp. 293–309, 1985.

[17] J. Meng, Y. Zhang, and L. Mei, "A virtual element method for the Laplacian eigenvalue problem in mixed form," *Applied Numerical Mathematics. An IMACS Journal*, vol. 156, pp. 1–13, 2020.

[18] P. L. Lederer, "A note on asymptotically exact a posteriori error estimates for mixed Laplace eigenvalue problems," *arXiv preprint arXiv:2204.03252*, 2022.

[19] S. Lu and X. Xu, "A geometrically consistent trace finite element method for the Laplace-Beltrami eigenvalue problem," *Surfaces*, vol. 58, no. 78, p. 59, 2021.

[20] M. A. Olshanskii, A. Reusken, and J. Grande, "A finite element method for elliptic equations on surfaces," *SIAM Journal on Numerical Analysis*, vol. 47, no. 5, pp. 3339–3358, 2009.

[21] F. Luo, Q. Lin, and H. Xie, "Computing the lower and upper bounds of Laplace eigenvalue problem: by combining conforming and nonconforming finite element methods," *Science China Mathematics*, vol. 55, no. 5, pp. 1069–1082, 2012.

[22] X. Liu and S. Oishi, "Verified eigenvalue evaluation for the Laplacian over polygonal domains of arbitrary shape," *SIAM Journal on Numerical Analysis*, vol. 51, no. 3, pp. 1634–1654, 2013.

[23] P. Monk and Y. Zhang, "An HDG method for the Steklov eigenvalue problem," *IMA Journal of Numerical Analysis*, 2021.

[24] J. Liu, J. Sun, and T. Turner, "Spectral indicator method for a non-selfadjoint Steklov eigenvalue problem," *Journal of Scientific Computing*, vol. 79, no. 3, pp. 1814–1831, 2019.

[25] M. G. Armentano and A. L. Lombardi, "The Steklov eigenvalue problem in a cuspidal domain," *Numerische Mathematik*, vol. 144, no. 2, pp. 237–270, 2020.

[26] Q. Li, Q. Lin, and H. Xie, "Nonconforming finite element approximations of the Steklov eigenvalue problem and its lower bound approximations," *Applications of Mathematics*, vol. 58, no. 2, pp. 129–151, 2013.

[27] D. Mora, G. Rivera, and R. Rodríguez, "A posteriori error estimates for a virtual element method for the Steklov eigenvalue problem," *Computers & Mathematics with Applications*, vol. 74, no. 9, pp. 2172–2190, 2017.

[28] D. Mora, G. Rivera, and R. Rodríguez, "A virtual element method for the Steklov eigenvalue problem," *Mathematical Models and Methods in Applied Sciences*, vol. 25, no. 08, pp. 1421–1445, 2015.

[29] H. Bi, S. Ren, and Y. Yang, "Conforming finite element approximations for a fourth-order Steklov eigenvalue problem," *Mathematical Problems in Engineering*, vol. 2011, 2011.

[30] A. B. Andreev and T. D. Todorov, "Isoparametric finite-element approximation of a Steklov eigenvalue problem," *IMA Journal of Numerical Analysis*, vol. 24, no. 2, pp. 309–322, 2004.

[31] F. Xu, M. Yue, Q. Huang, and H. Ma, "An asymptotically exact a posteriori error estimator for non-selfadjoint Steklov eigenvalue problem," *Applied Numerical Mathematics*, vol. 156, pp. 210–227, 2020.

[32] M. Yue, F. Xu, and M. Xie, "A multilevel Newton's method for the Steklov eigenvalue problem," *Advances in Computational Mathematics*, vol. 48, no. 3, pp. 1–29, 2022.

[33] Ö. Türk, "A DRBEM approximation of the Steklov eigenvalue problem," *Engineering Analysis with Boundary Elements*, vol. 122, pp. 232–241, 2021.

[34] F. Aboud, F. Jauberteau, G. Moebs, and D. Robert, "Numerical approaches for some nonlinear eigenvalue problems," *arXiv preprint arXiv:1608.06182*, 2016.

[35] A. Carasso, "Finite-difference methods and the eigenvalue problem for non-selfadjoint Sturm-Liouville operators," *Mathematics of Computation*, vol. 23, no. 108, pp. 717–729, 1969.

[36] R. A. Usmani, "Finite difference methods for computing eigenvalues of fourth order boundary value problems," *International Journal of Mathematics and Mathematical Sciences*, vol. 9, no. 1, pp. 137–143, 1986.

[37] M. Chawla and P. Shivakumar, "A symmetric finite difference method for computing eigenvalues of Sturm-Liouville problems," *Computers & Mathematics with Applications*, vol. 26, no. 2, pp. 67–77, 1993.

[38] S. Sajavcius, "On the eigenvalue problems for finite-difference operators with coupled boundary conditions.," in *Siauliai Mathematical Seminar*, vol. 5, 2010.

[39] N. O'Brien, K. Djidjeli, and S. J. Cox, "Solving an eigenvalue problem on a periodic domain using a radial basis function finite difference scheme," *Engineering Analysis with Boundary Elements*, vol. 37, no. 12, pp. 1594–1601, 2013.

[40] J. R. Kuttler, "Finite difference approximations for eigenvalues of uniformly elliptic operators," *SIAM Journal on Numerical Analysis*, vol. 7, no. 2, pp. 206–232, 1970.

[41] J. Kuttler, "Upper and lower bounds for eigenvalues by finite differences," *Pacific Journal of Mathematics*, vol. 35, no. 2, pp. 429–440, 1970.

[42] L. Veidinger, "A finite difference method for evaluating the eigenvalues and eigenfunctions of the Laplace operator," *USSR Computational Mathematics and Mathematical Physics*, vol. 6, no. 4, pp. 103–119, 1966.

[43] S. Yıldırım, "Exact and numerical solutions of Poisson equation for electrostatic potential problems," *Mathematical Problems in Engineering*, vol. 2008, 2008.

[44] H. N. Gharti and J. Tromp, "A spectral-infinite-element solution of Poisson's equation: an application to self gravity," *arXiv preprint arXiv:1706.00855*, 2017.

[45] E. Deriaz, "Compact finite difference schemes of arbitrary order for the Poisson equation in arbitrary dimensions," *BIT Numerical Mathematics*, vol. 60, no. 1, pp. 199–233, 2020.

[46] D. Boffi, "Finite element approximation of eigenvalue problems," *Acta Numerica*, vol. 19, pp. 1–120, 2010.

[47] E. Bahadır, "Approximation of eigenvalue problems using finite element methods," Master's thesis, Gebze Technical University, 2021.